Online LTP Seminar
September 15th, 2020

Plasma enabled heterogeneous catalysis for greenhouse gas conversion: kinetic modeling

Tomohiro Nozaki

Tokyo Institute of Technology
Dept Mechanical Engineering

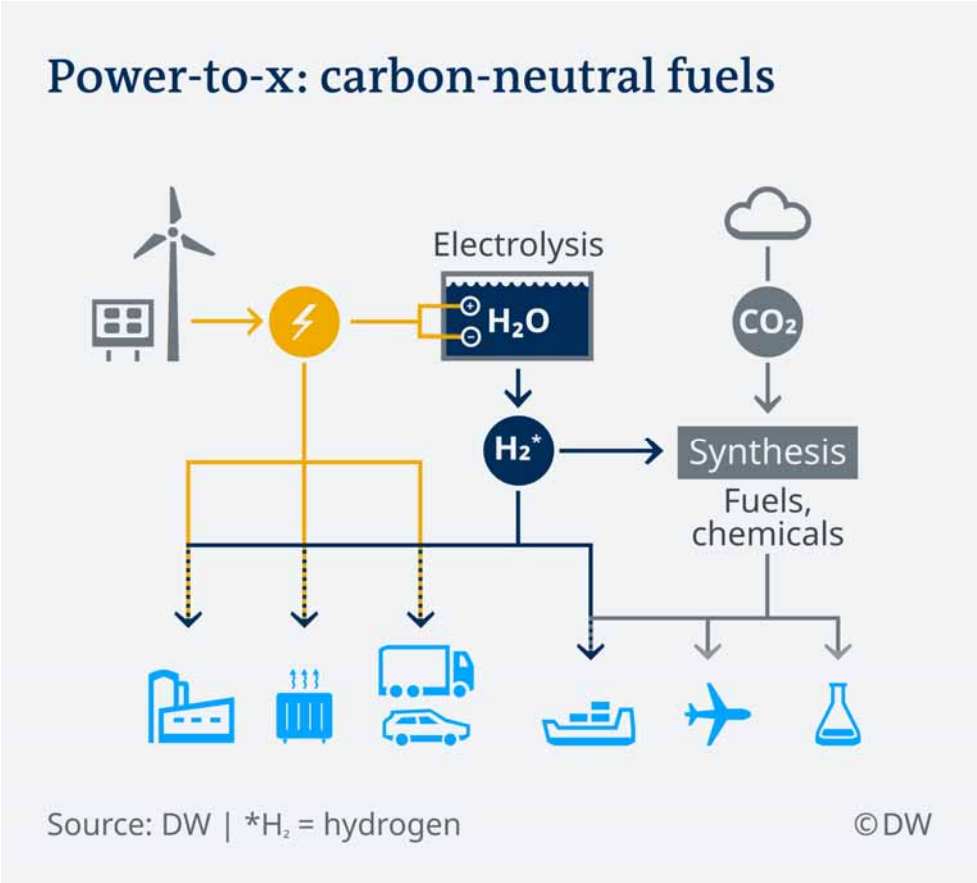

https://www.dw.com/en/power-to-x-the-secret-to-a-100-renewable-energy-system/a-51662014

Electrochemistry + Photochemistry and Plasma chemistry

https://www.voltachem.com/research/power-2-chemicals

Power-to-X Roadmap

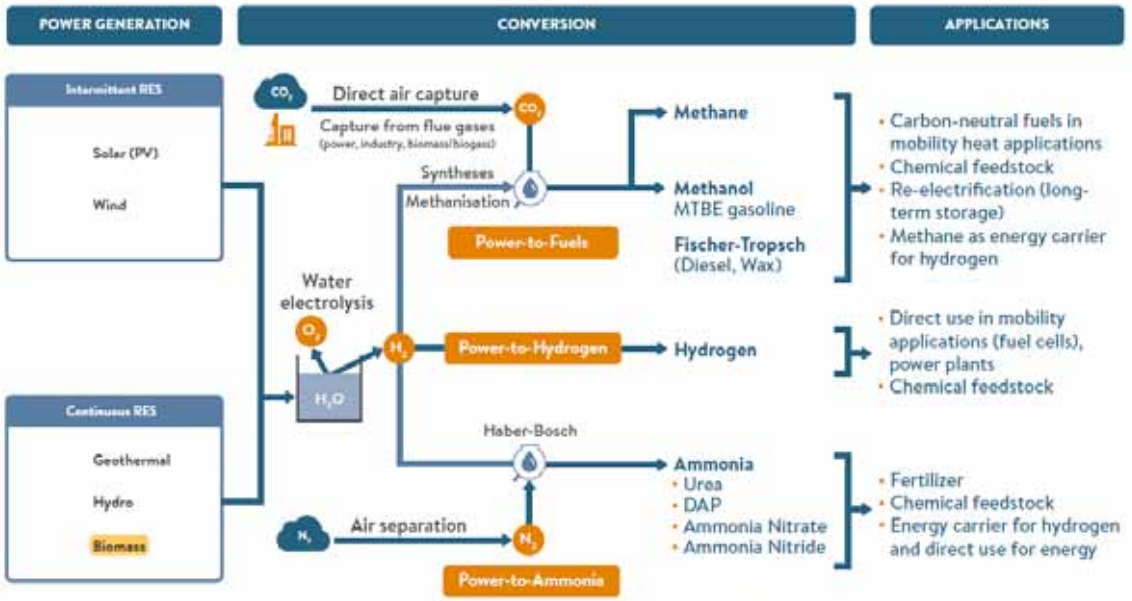

Source: International aspects of a power-to-x roadmap, Weltenergierat Deutschland, 2018

ref. International aspects of a power-to-x roadmap, Weltenergierat Deutschland, 2018

Power-to-fuel
- Power-to-chemicals
- Power-to-gas
- Power-to-syngas
- Power-to-methane
- Power-to-liquid

Power-to-hydrogen

Power-to-ammonia

Power-to-heat

Power-to-mobility

Power to food

power-to-power (wiki)

Photocatalysis, Photoelectrochemical, Plasmonic Photosynthesis, Hot carriers, etc

Principle is relatively well-known

Development of functional materials.

TiO_2: *n*-type

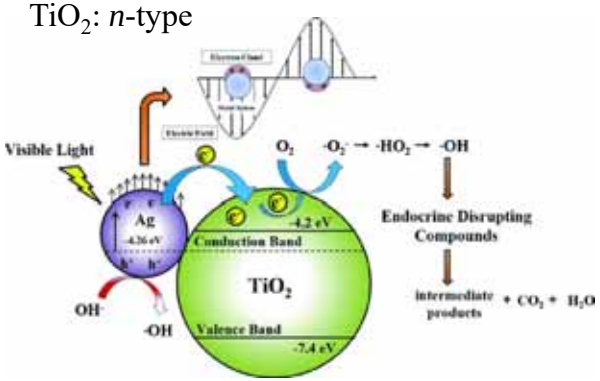

Leon et al: DOI 10.1007/978-3-319-48009-1_9 (2016)

Amano et al, *ACS Energy Lett.* **4**, 502 (2019)

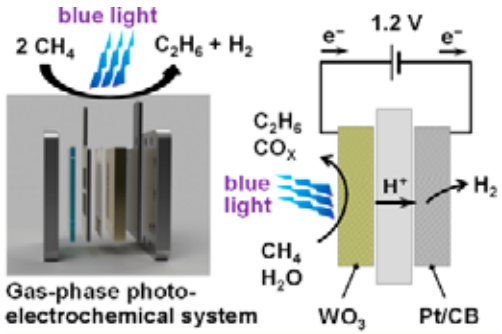

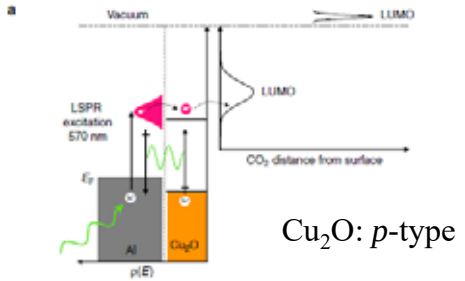

Cu_2O: *p*-type

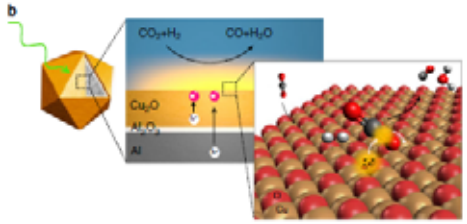

Robatjazi et al, *Nature comm.* **8**:27 (2017)

What is plasma catalysis ?

- Nonthermal plasma + heterogeneous catalysts.
- Similarities btw plasma-enhanced CVD, Atomic layer processes, etc.
- Too complex to understand.

We also need material (catalyst) development based on known principle.

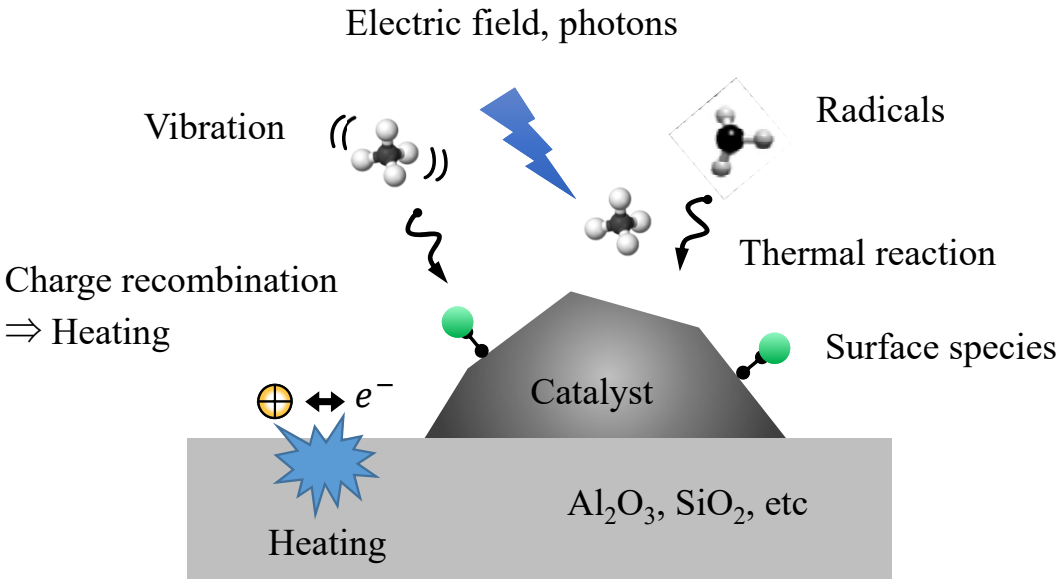

$Ne \sim N_{ion}$

$N_{CH3} \sim 10Ne$

$N_{vib} \sim 100Ne$

T Nozaki et al: *Catal. Today* **89** (2004) 57.

T Nozaki et al: *J Phys D*, **52** (2019) 414002.

Reactivity of vibrationally excited CH_4

IR laser: mode selective activation to asymmetric vibration (ν_3 = 0.36 eV)

*E*t: Translational energy
hn_3: Vibrational energy

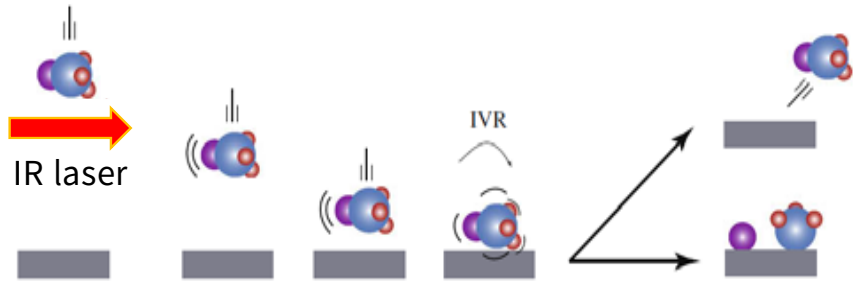

IVR: Intramolecular vibrational redistribution

A L Utz: *Curr. Opin. Solid St M*, **13** (2009) 4–12.

Rate-limiting step: $CH_4 = CH_3^* + H^*$

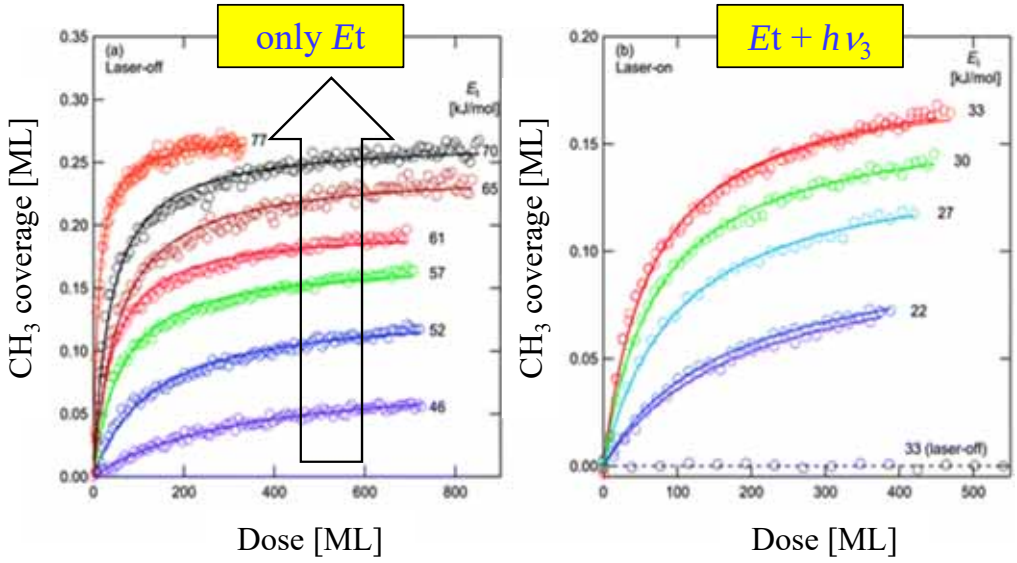

- Pt (111) @ 150 K, 10^{-5} Pa.
- Ultra-high vacuum (< 10^{-5} Pa)
- Surface coverage increases with increasing (*E*t).
- Vibrational energy (hn_3) increase coverage at much smaller *E*t.

1 ML (monolayer): Pt(111), 1.51×10^{15} atoms/cm^2

H Ueta et al: *Phys. Chem. Chem. Phys.*, **15** (2013) 20526.

Initial sticking probability and Saturated surface coverage

Vibrational excitation

$E_t + h\nu_3$

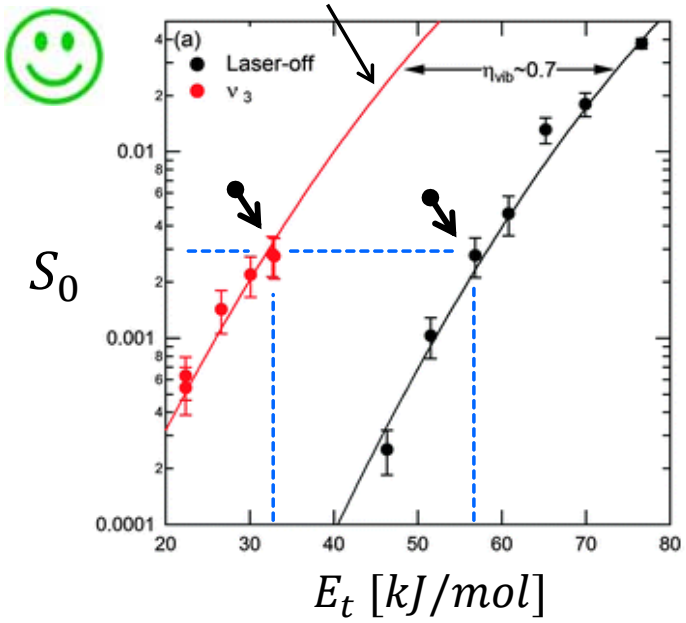

Total Energy

($Et + h\nu_3$) = 68 kJ/mol > Et = 58 kJ/mol

Asymmetric vibration + Pt (111) @ 150 K

- Energy inefficient ~ 70%
- But low temperature reactivity is enhanced.

H Ueta et al: *Phys. Chem. Chem. Phys.*, **15** (2013) 20526.

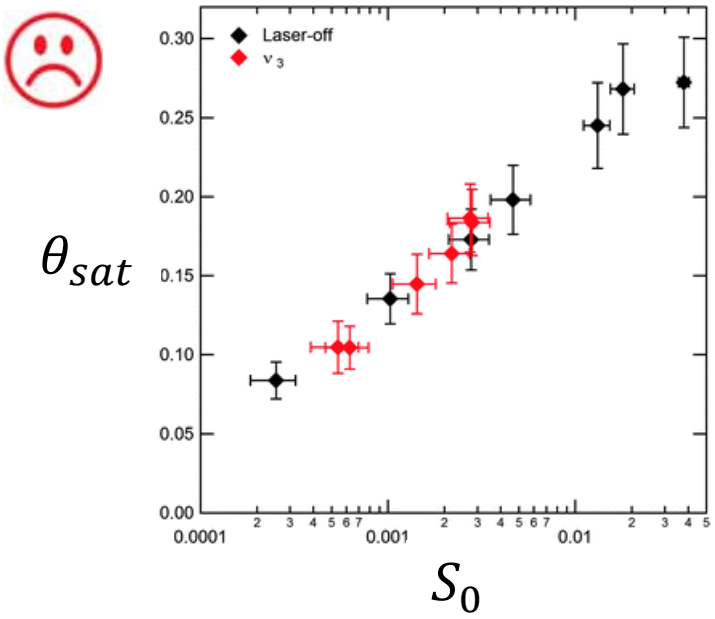

θ_{sat}~30%

- Steric interference between surface CH_3^*
- θ_{sat}: not increase by vibration.

Typical Langmuir type absorption behavior

H Ueta et al: *Phys. Chem. Chem. Phys.*, **15** (2013) 20526.

Co-reactants: oxidize CH*x** and regenerate active sites.

30% -- CH_3*
30% -- H*
40% -- vacancy (permanently)

ex. particles with surface ligands

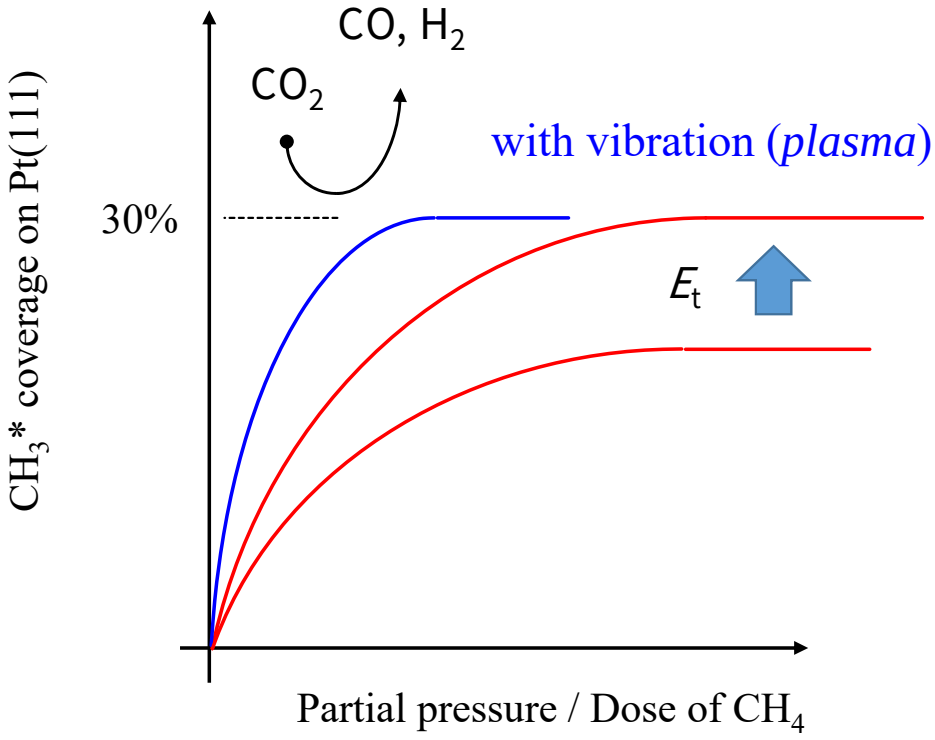

Saturation ~ up to 30% over Pt(111)
unchanged by vibration !

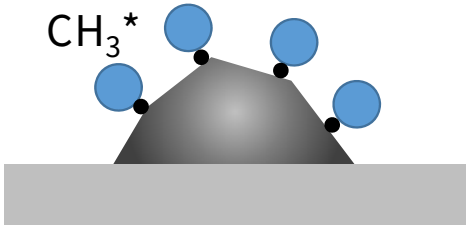

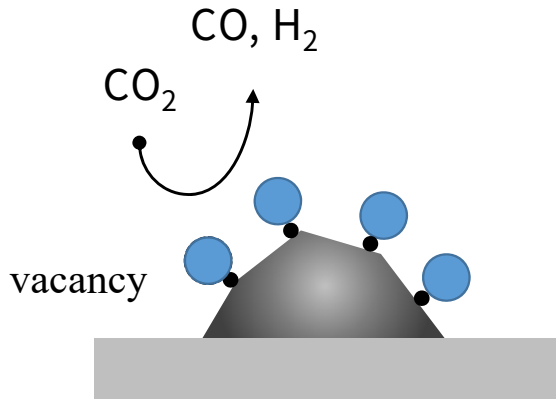

Ni/Al_2O_3 catalyst

$$CH_4 + CO_2 = 2CO + 2H_2$$

Kameshima et al, *Plasma Process. Polym.*, **14**, (2017) e01600096.

☹ CH_4 conversion was not increased by DBD.

☺ CO_2 conversion increased slightly, contributing more syngas and less coking.

3 mm

Plasma catalysis

Carbon is a footprint of the reaction

Thermal catalysis

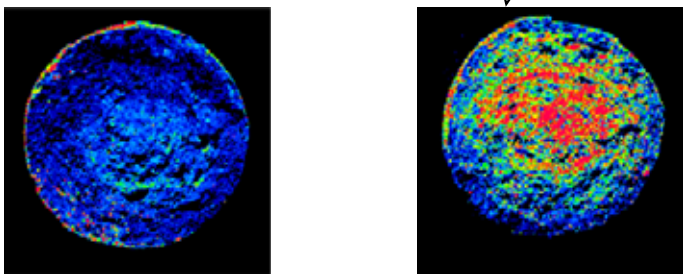

466°C

465°C

Carbon mapping by *EPMA* (Electron probe micro analyzer)

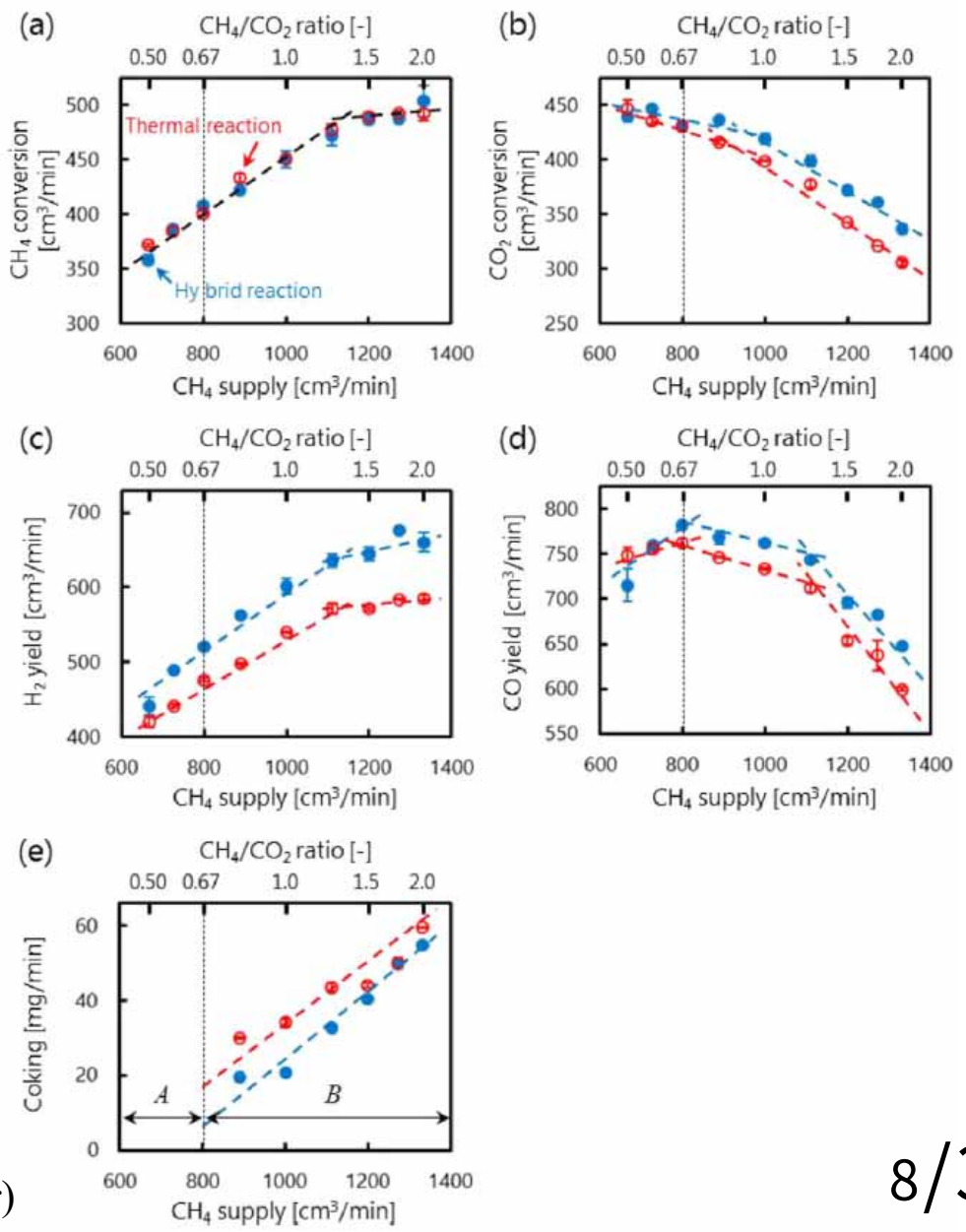

Plasma-induced modification of catalyst (Ni to NiO): tentatively, $CO_2{}^v$ plays a role

Snoeckx and Bogaerts: *Chem. Soc. Rev.*, **46** (2017) 5805.

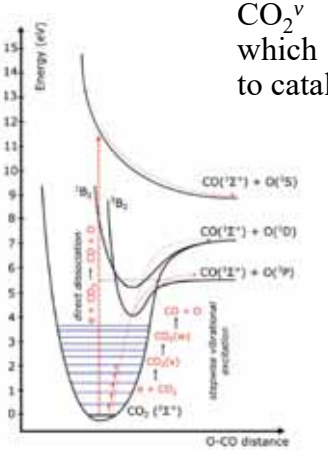

$CO_2{}^v$ is energy reservoir which transfer their energy to catalysts.

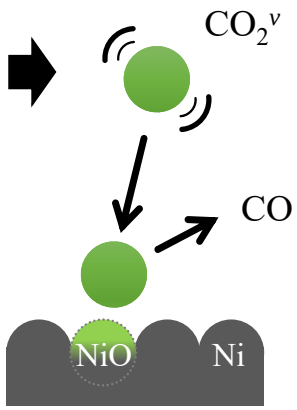

Catalyst modification

- Formation of NiO is possible only when DBD is applied.
- NiO uptakes surface oxygen beyond thermal equilibrium, enabling low coke formation.
- Catalyst activity of NiO is no as high s Ni.

Z. Sheng, *et al.*, *J. Phys. D: Appl. Phys.* **51** (2018) 445205

$$CO_2 + e \xrightarrow{DBD} CO_2{}^v + Ni \xrightarrow{surface} NiO$$

$$CO_2 + e \xrightarrow{DBD} CO + Ni \xrightarrow{surface} NiO$$

Thermal catalysis

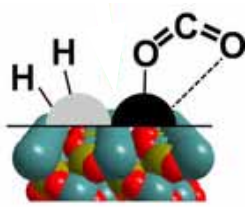

Plasma catalysis

C Weilach et al, *J. Phys. Chem. C*, 116 (2012) 18768.

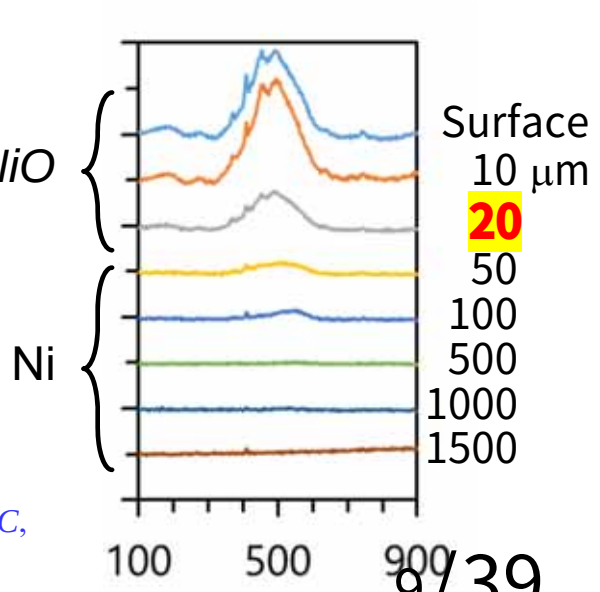

Nonthermal plasma in micropores ?

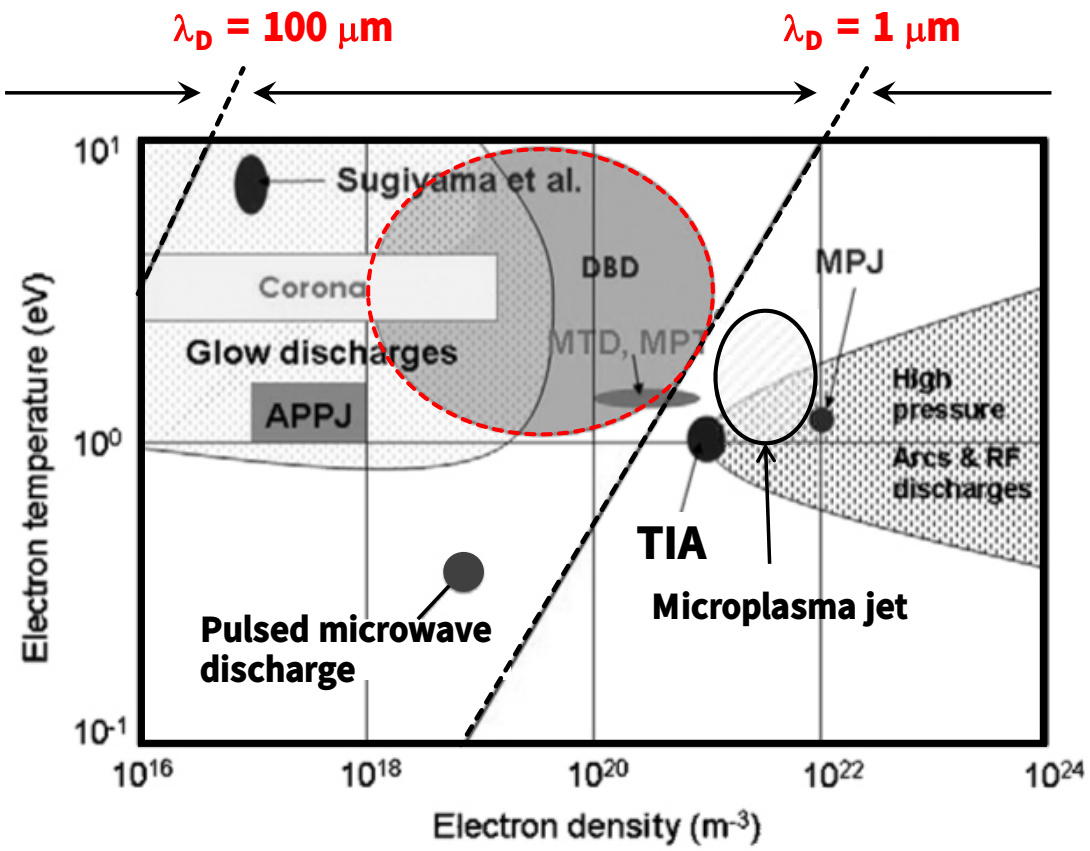

C Tendero *et al.*: *Spectrochimica Acta B*, **61** (2006) 2.

$$1\ \mu m < \text{Debye length (DBD)} < 100\ \mu m$$

$$\lambda_D = \sqrt{\frac{\varepsilon_0 \kappa T_e}{N_e e^2}} = 7.43 \times 10^3 \sqrt{\frac{T_e}{N_e}}$$

DBD cannot penetrate into pores smaller than 1 μm.

A Bogaerts et al, *Appl Catal B: Environ* **185** (2016) 56.

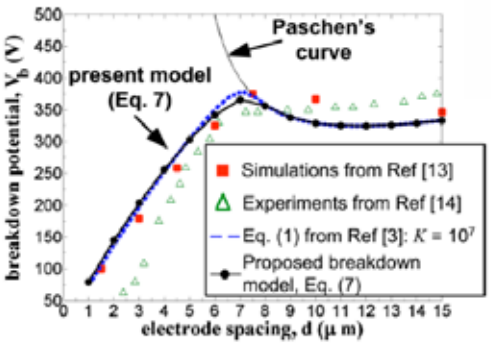

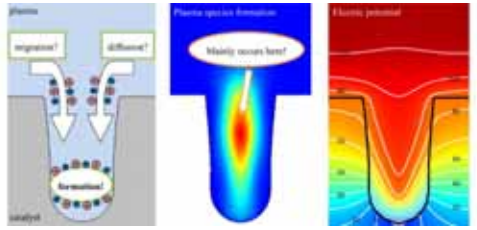

Gas breakdown does not occur in micropores.

R Tirumala and D B Go, *APL* **97** (2010) 151502
D B Go and A Venkattraman, *JPD* **47** (2014) 503001

New catalyst: La-modified Ni/Al_2O_3

La, K, Mg are know to produce carbonates from CO_2, enhancing surface oxygen species.

Z Sheng et al, *Phys. Chem. Chem. Phys.*, **22** (2020) 19349.

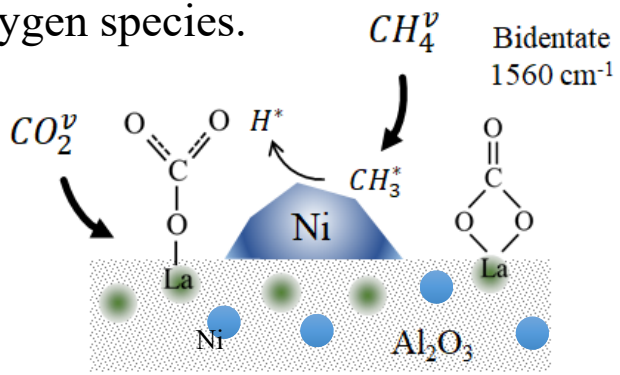

Ni

$Ni(12wt\%)/Al_2O_3$

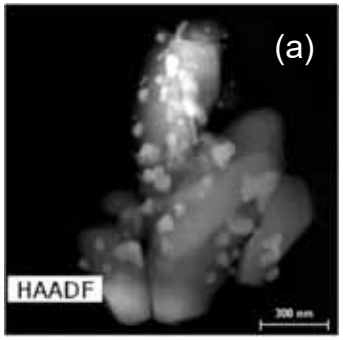

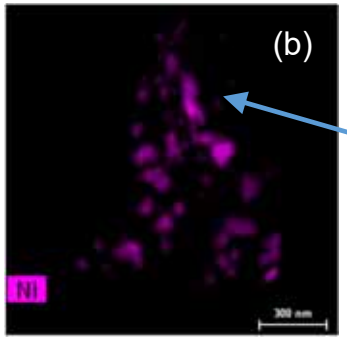

Particles
Ni: 29.0 nm
(Scherrer Eq)

La

overlap

$La(3wt\%)$-
$Ni(11wt\%)/Al_2O_3$

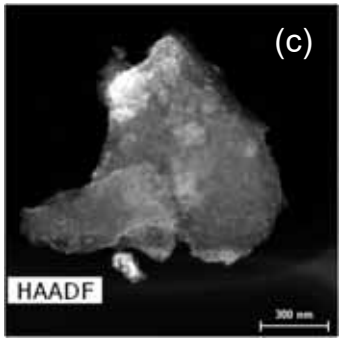

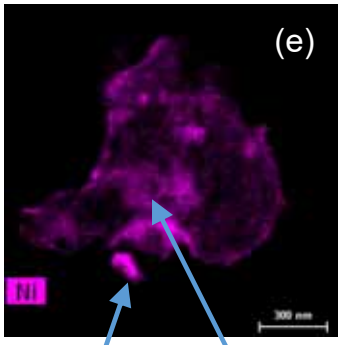

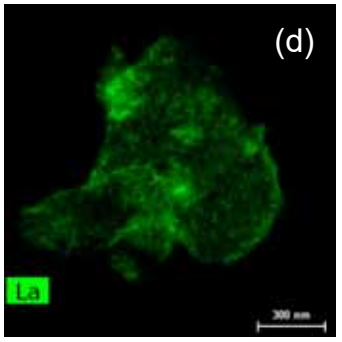

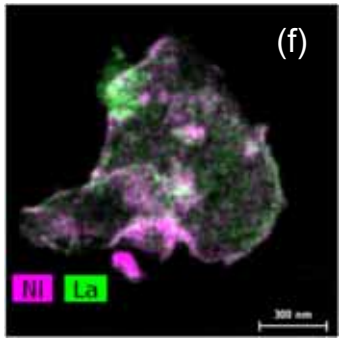

Particles Dots
Ni: 10.8 nm

Atomic weight
Ni: 59, La: 139

Representative results: pulsed reforming

$CH_4 + CO_2 = 2CO + 2H_2$

S Kameshima et al: *Catalysis Today*, **256** (2015) 67-75

$CH_4/CO_2 = 0.5$ ⟹ Stoichiometry $CH_4/CO_2 = 1.0$ ⟹ $CH_4/CO_2 = 1.5$

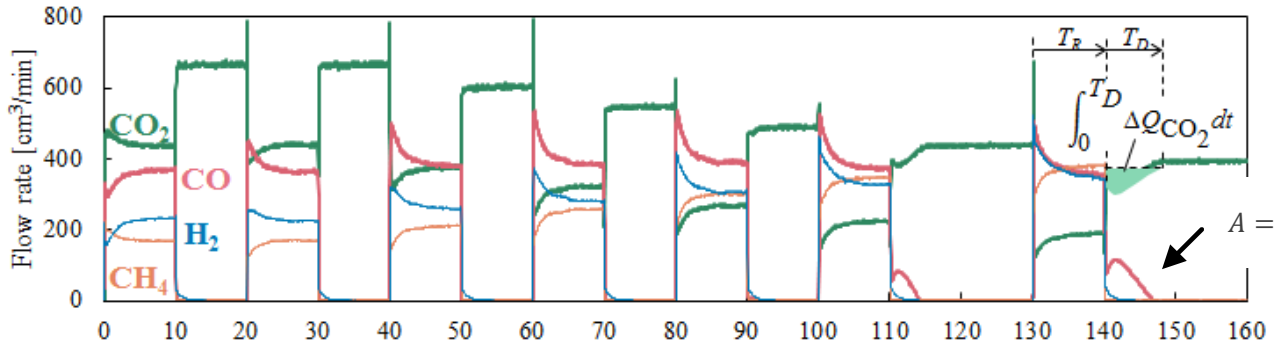

$C + CO_2 = 2CO$

Catalyst Temperature

Time (min) ⟶

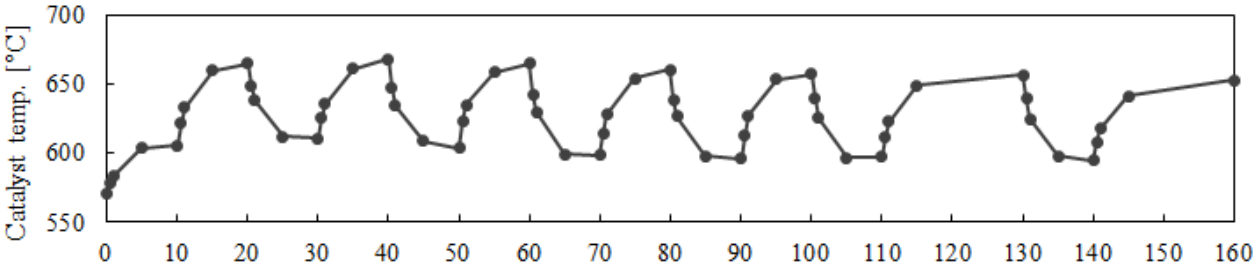

- *SEI* = 1.37 eV/molec.: avoid plasma heating and maximize energy efficiency.
- Frequency: 12 kHz and 100 kHz.

CH_4 *conv.*

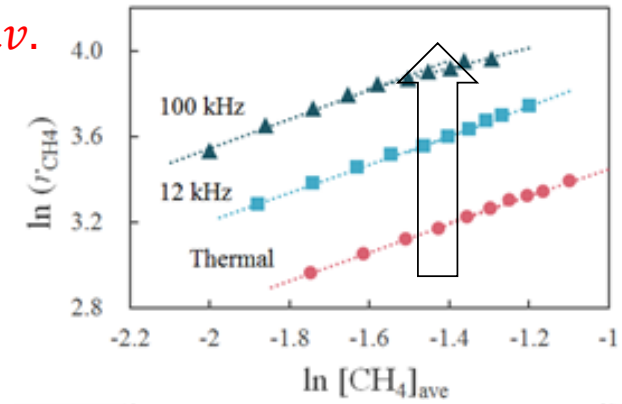

CO_2 *conv.*

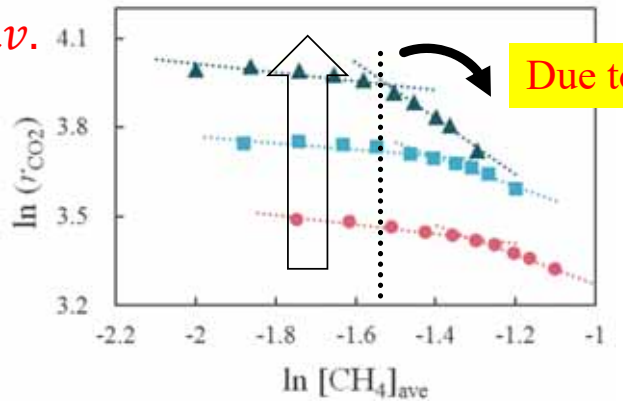

CO_2 activation is even more important !!

H_2 *yield*

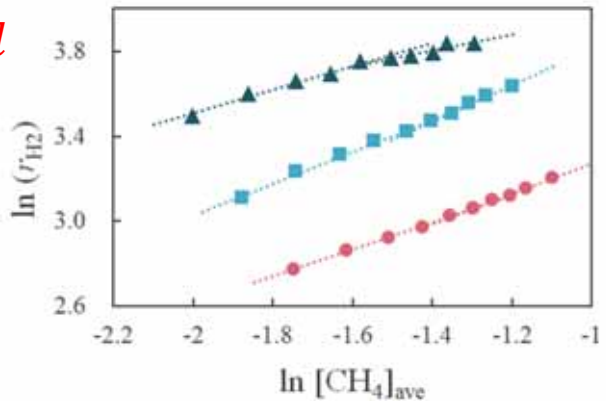

CO yield

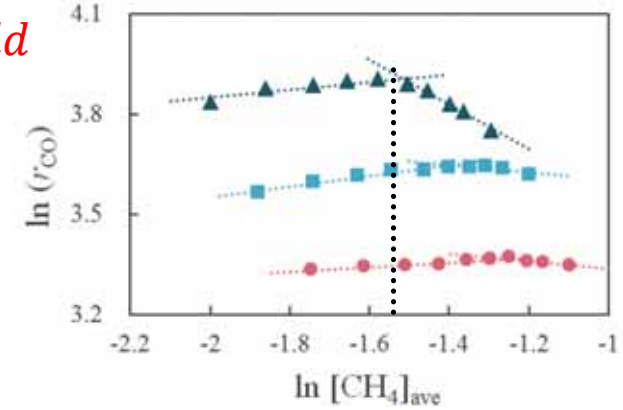

Monodentate carbonate: 1540 and 1370 cm^{-1}

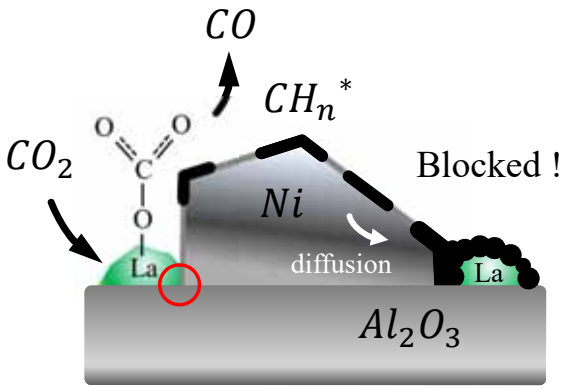

Coke yield

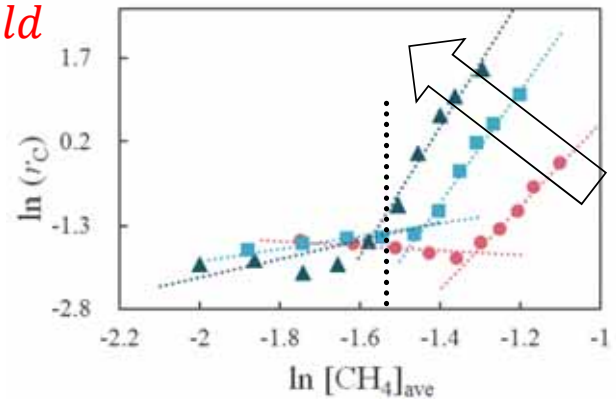

Reaction rate v.s. Mean CH_4 partial pressure

$$r_i = \frac{\Delta C_i}{\Delta t} = \frac{C_i^{in} - C_i^{out}}{\Delta t}$$

Temp = 600 °C fixed

Sheng et al: *J Phys D*, **52** (2019) 414002.

in situ DBD-DRIFTS

(Diffuse reflectance infrared fourier transform spectroscopy)

(operating temperature range: 0–200°C)

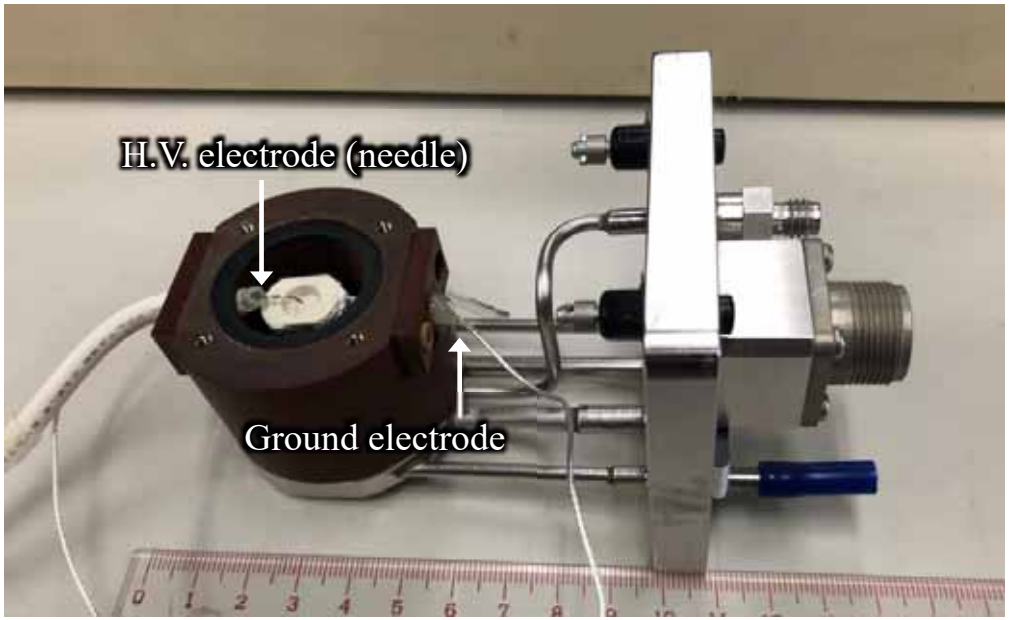

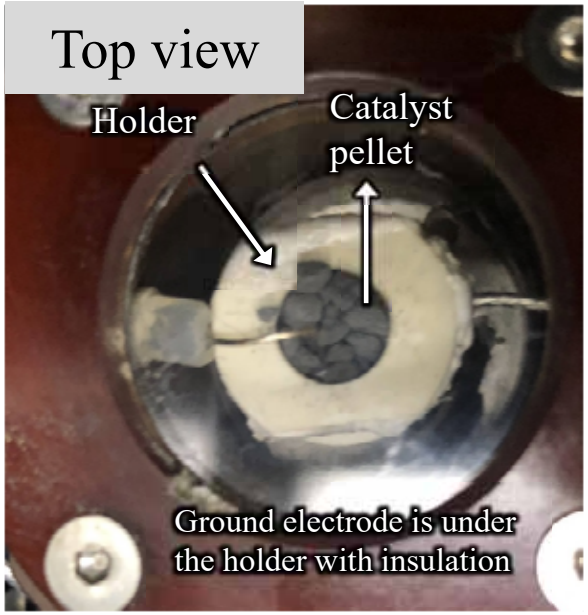

Z Sheng et al, *Phys. Chem. Chem. Phys.*, **22** (2020) 19349-19358.

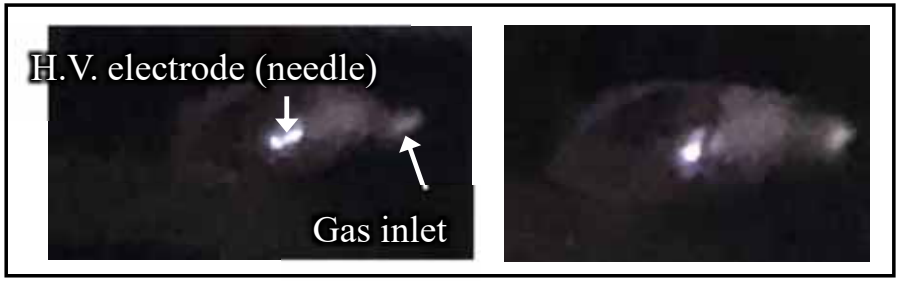

N Turan et al, *J. Phys. D: Appl. Phys.* **53** (2020) 275201.

S Zhang et al, *J. Phys. D: Appl. Phys.* **53** (2020) 215201.

Formation of carbonates on La

Z Sheng et al, *Phys. Chem. Chem. Phys.*, **22** (2020) 19349.

$Ni(12wt\%)/Al_2O_3$

Carbonate peak is negligible.

$La(3wt\%)\text{-}Ni(11wt\%)/Al_2O_3$

Strong carbonate peaks which is further enhanced by DBD.

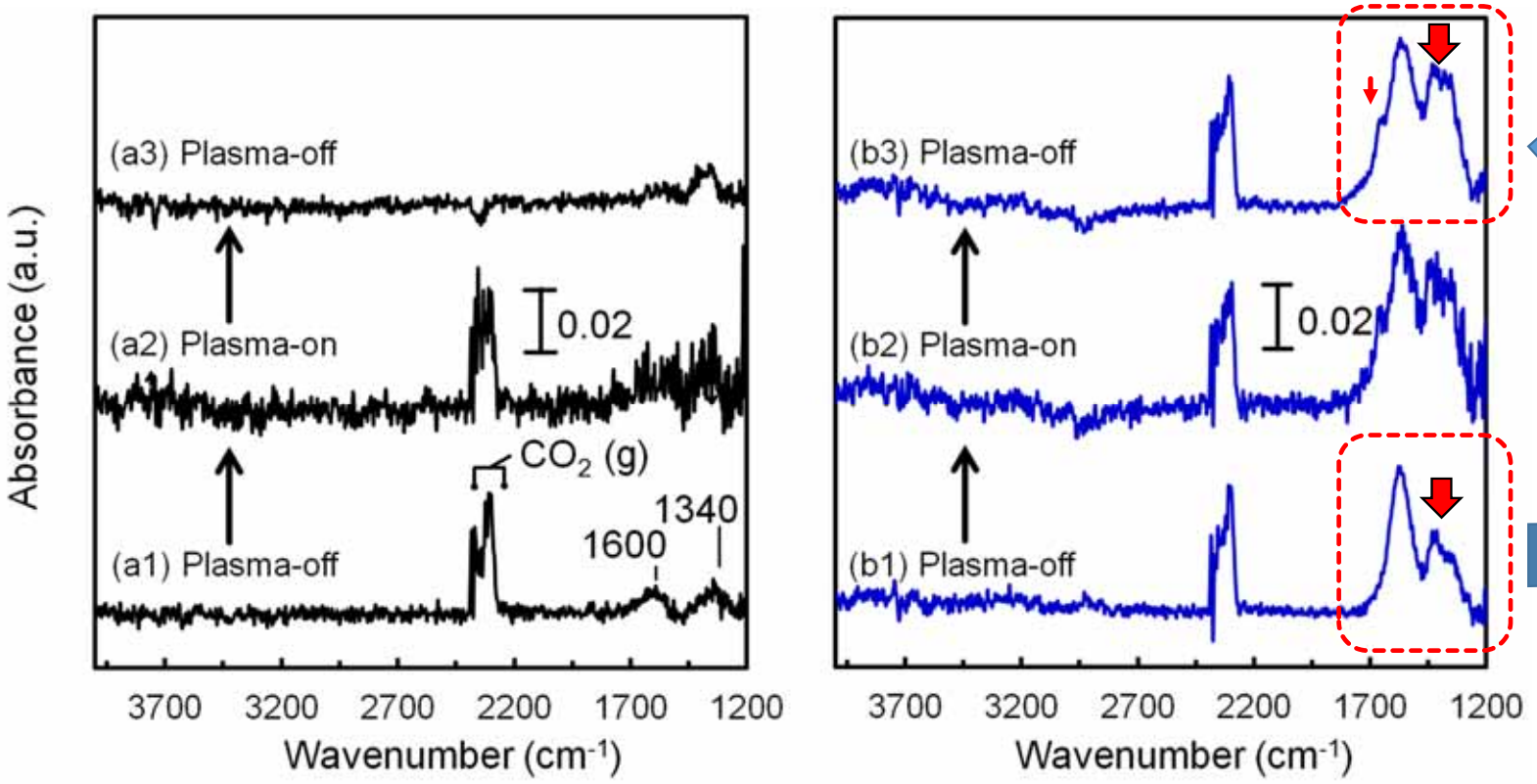

Enlarged spectrum on next page

Fingerprint region

Enlarged spectrum 1200~1800 cm^{-1}

Z Sheng et al, *Phys. Chem. Chem. Phys.*, **22** (2020) 19349.

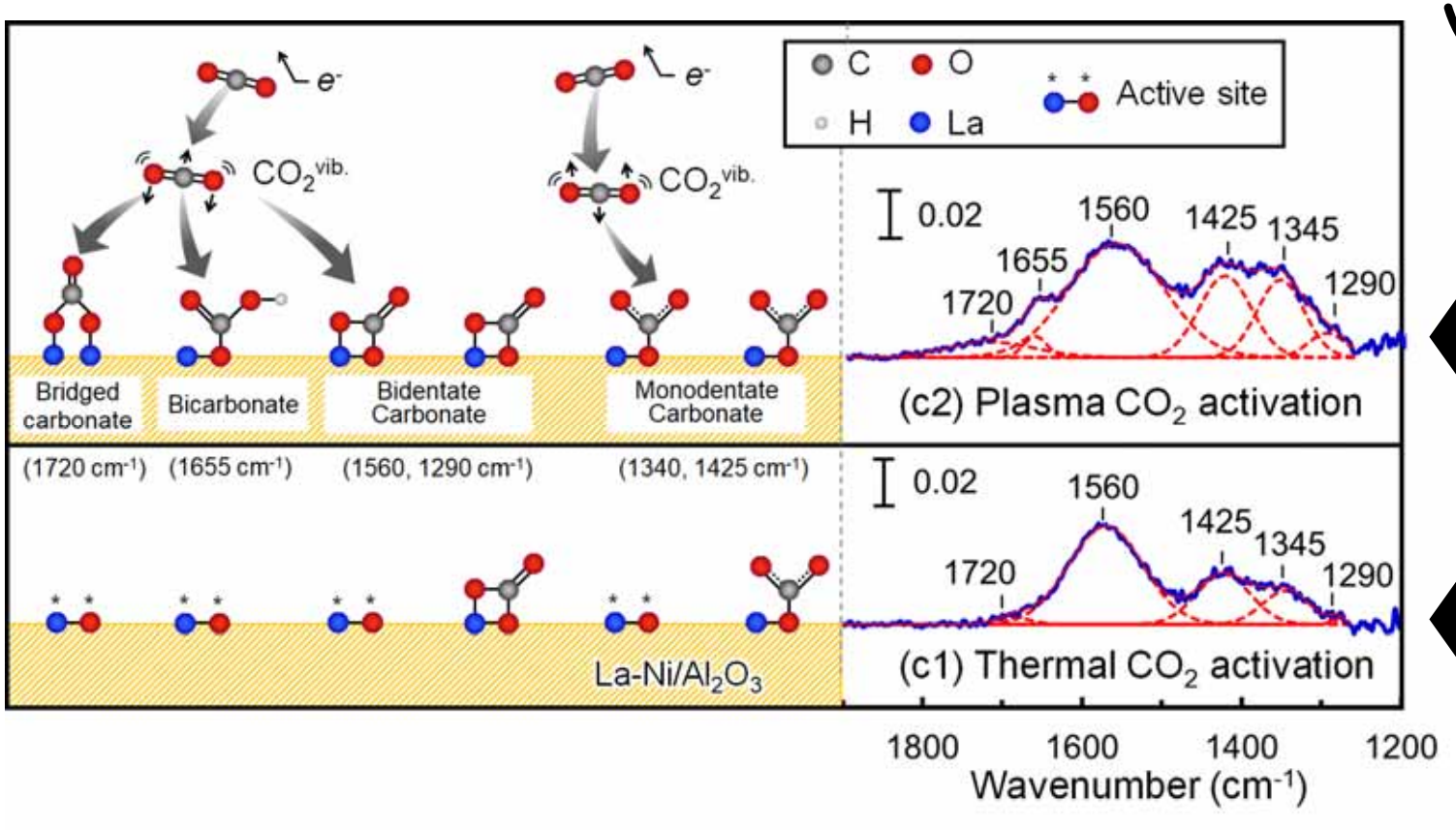

Monodentate carbonate:
1540 and 1370 cm^{-1}

CH_4^v

Bidentate
1560 cm^{-1}

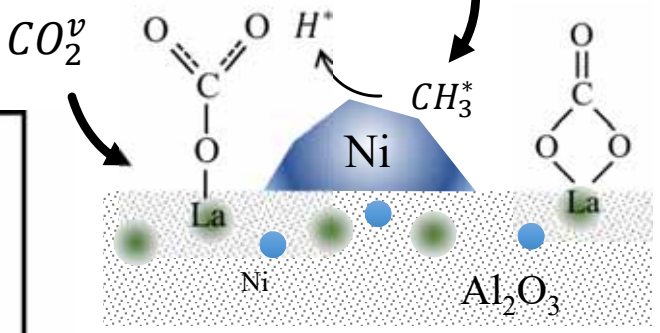

Plasma

Thermal

overlap

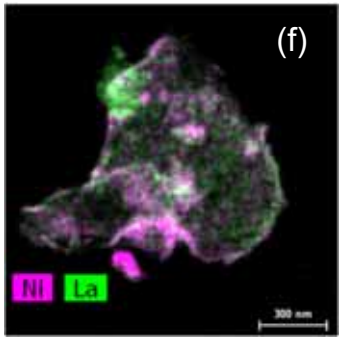

- La-Ni/Al2O3 is highly suitable for DBD hybrid reaction.
- Appropriate catalysts must be combined
- 100 kHz is better than 12 kHz.

Kinetic analysis

Reaction order, Arrhenius plot, Activation energy

$$CH_4 + CO_2 = 2CO + 2H_2$$

$$La{:}Ni/Al_2O_3$$

Packed-bed DBD

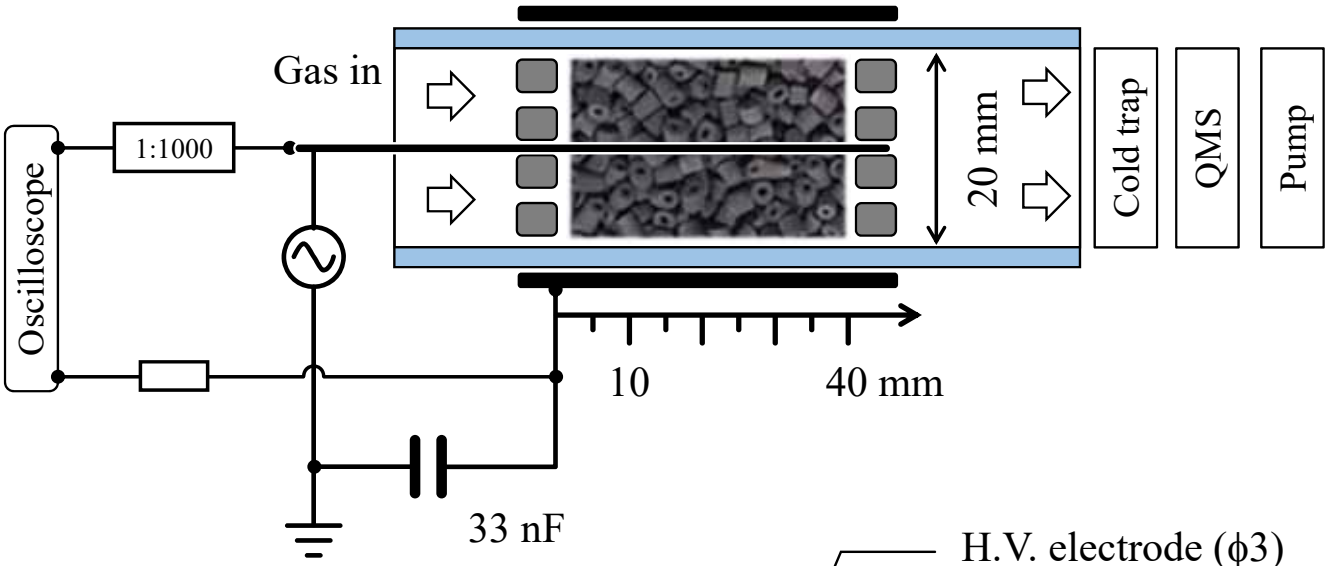

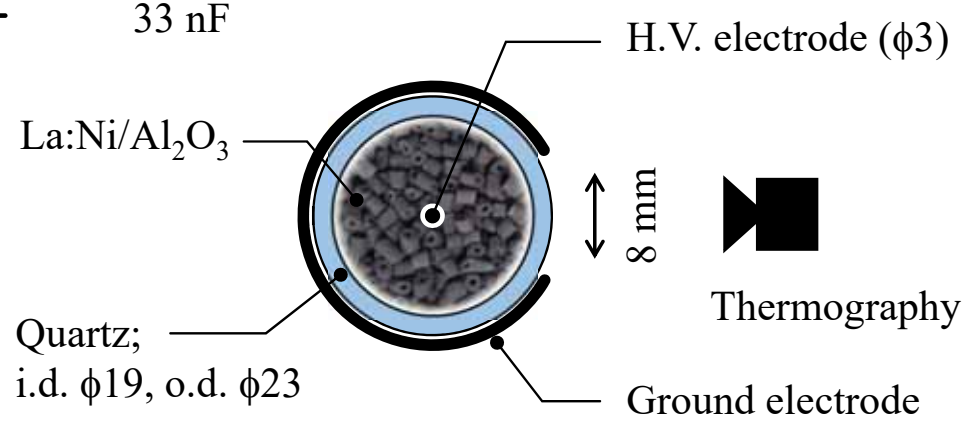

3wt%La-11wt%Ni/Al_2O_3

- Gas flow rate: 1000 cm^3/min
- Pressure: 5 kPa
- Temp.: 400~700 °C
- Power: 90 W
- *SEI*: 1.3~2.0 eV/molecule
- *GHSV*: 10,000 h^{-1}

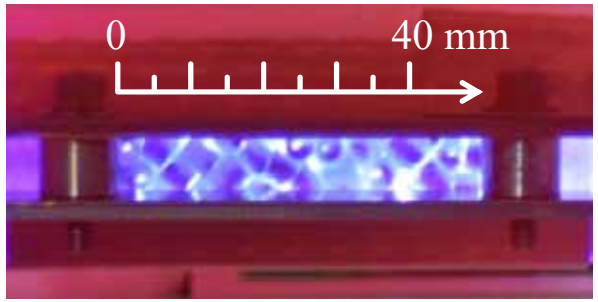

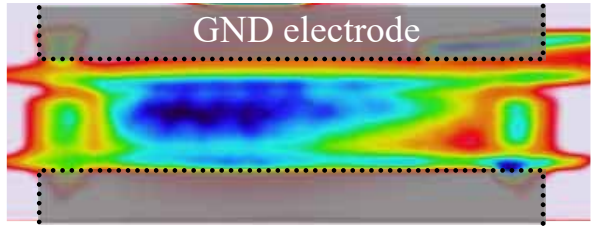

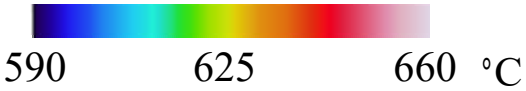

Key parameters

X. Tu, J.C. Whitehead, T. Nozaki (Ed.)
Plasma catalysis: fundamentals and applications, Springer, Cham (2019)

SEI (Specific Energy Input) $$SEI\ (eV/molecule) \propto \frac{P\ (W)}{Q\ (cm^3/min)}$$ at STP

$$CH_4 + CO_2 = 2CO + 2H_2 \qquad \Delta H = 247\ \text{kJ/mol} = 2.56\ eV/molecule$$

* Specific Energy Requirement (*SER*)

SEI < *SER* (= 2.56 eV/molecules)

GHSV (Gaseous Hourly Space Velocity) $$GHSV(h^{-1}) \propto \frac{Q\ (cm^3/min)}{V\ (cm^3)}$$

GHSV > 1,000 h^{-1}

Power density (W/cm^3) = *SEI* × *GHSV*

WHSV (Weight Hourly Space Velocity) $$WHSV(h^{-1}) = \frac{Q\ (g/h)}{mass\ (g)}$$

Arrhenius plot for the apparent activation energy

$$r = -\frac{\mathrm{d}[CH_4]}{\mathrm{d}t} = k_f[CH_4]^{0.63}[CO_2]^{-0.17}$$

FACTS

- Reaction order was kept unchanged by DBD.
  → Assume L-H mechanism, reaction order represents surface coverage which was not influenced by DBD: absorption is fast, but saturation is kept unchanged.

Reaction rate ↑, k_f ↑ !!

Sheng et al, *Chem Eng J*, **399** (2020.) 125751.
See also *Supporting Information*.

Ground state CH_4 (Thermal catalysis)	Vibrationally excited CH_4 (Plasma catalysis)
$k_f = Ae^{-\frac{E_t}{RT}}$	$k_f = Ae^{-\frac{E_t-\eta E_v}{RT}}$
	$1 < \eta$
E_t = 91.0 kJ/mol	E_t = 44.7 kJ/mol

experiments wit

Conditions & Gas input profile

Flow rate	CH_4 / CO_2 = 0.8
GHSV [h^{-1}]	5,000
Pressure [kPa]	5

Input power [W]	88 – 91
SEI [eV/molecule]	1.37
Catalyst	La:Ni/Al_2O_3

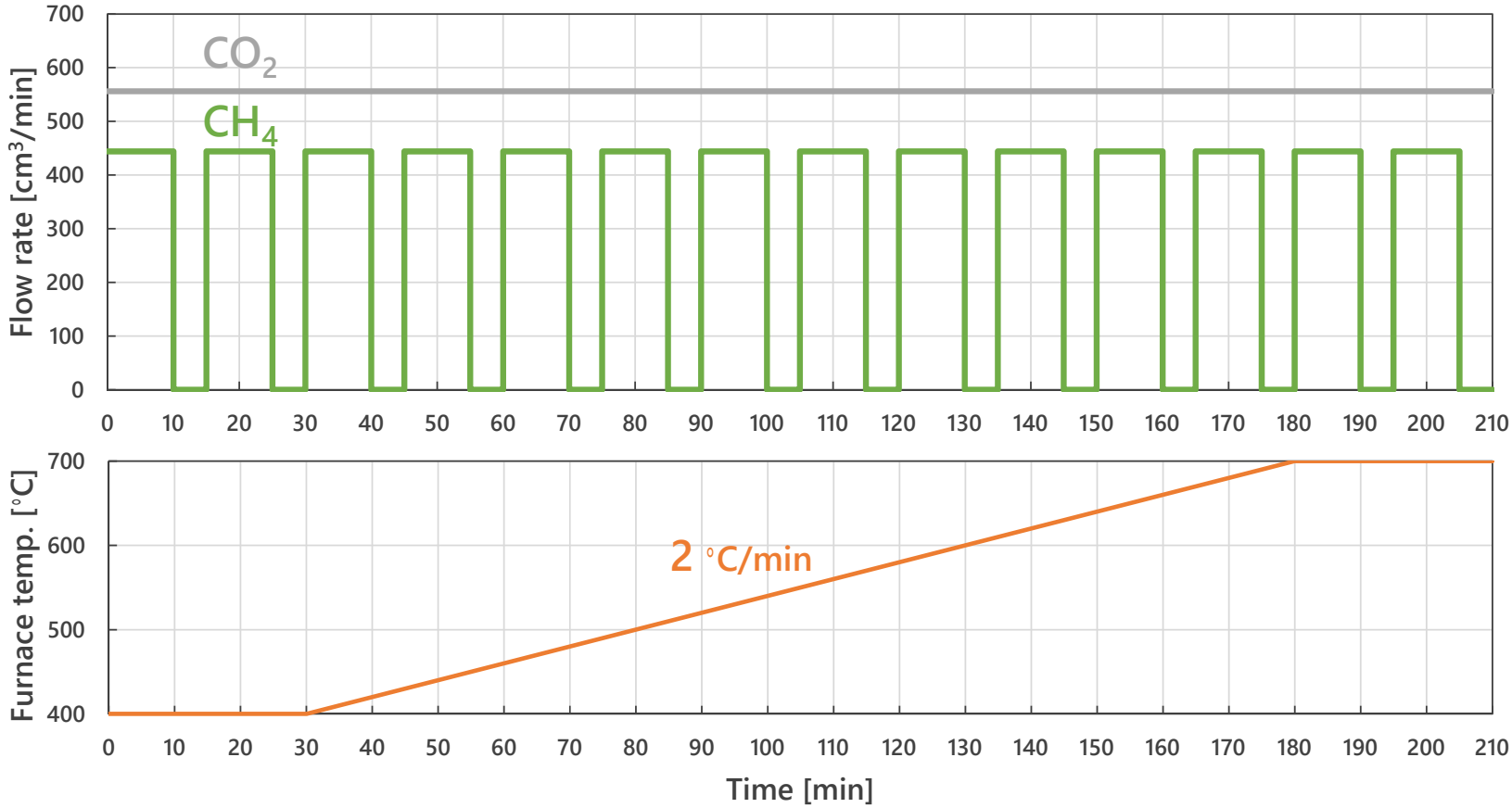

Results: 400 ~ 700 °C (*Plasma catalysis@ 100 kHz DBD*)

No coking confirmed.

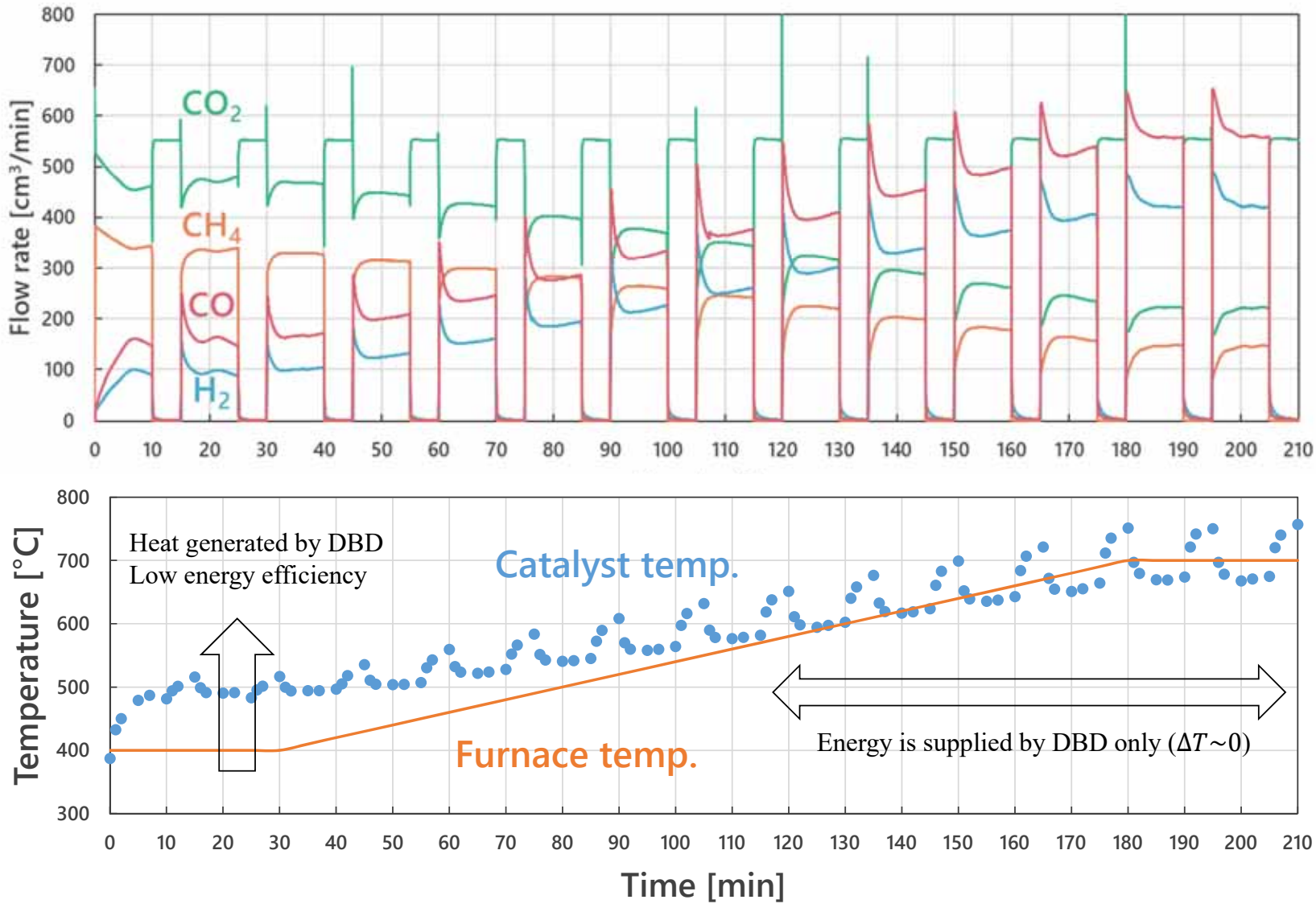

$$r_{CH_4}{}' = r_{CH_4}\left(1 - \frac{1}{K_e}\frac{{P_{CO}}^2 {P_{H_2}}^2}{P_{CH_4}P_{CO_2}}\right)$$

Arrhenius plot for activation energy

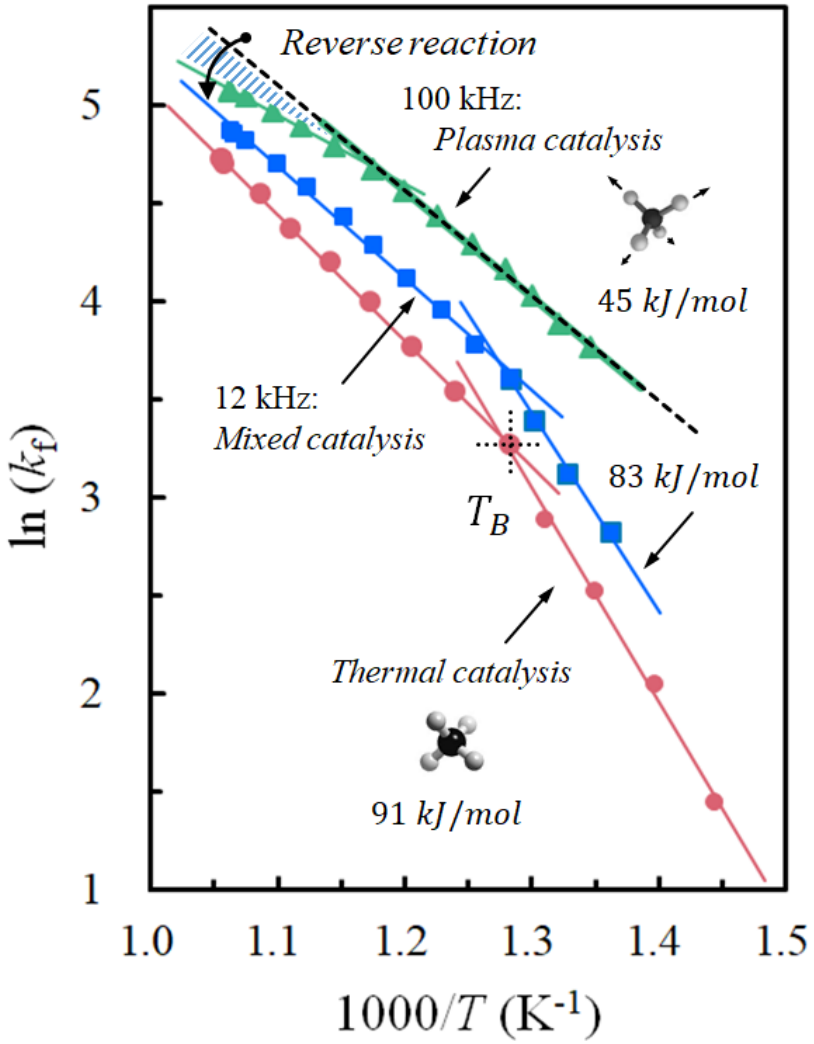

H-H Kim et al: *J Phys D*, **49** (2016) 415204

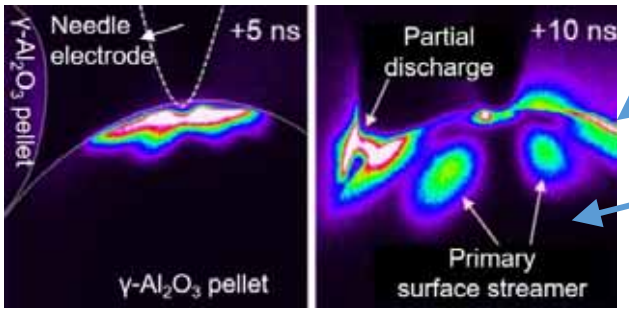

Streamer: hybrid reaction

Thermal reaction

Ag/Al_2O_3 in Air

Mixed catalysis
(12 kHz DBD)

$T > T_B = 510$ °C $\quad r_{app} \propto \sqrt{k_f D} \propto e^{-\frac{E_t/2}{RT}}$

E_t is halved due to the mass transfer resistance in micropores, known as "*catalyst effectiveness factor*".

Modified activation energy due to vibrational excitation

The rate-determining step: $CH_4 \rightarrow CH_4^* \rightarrow CH_3^* + H^*$

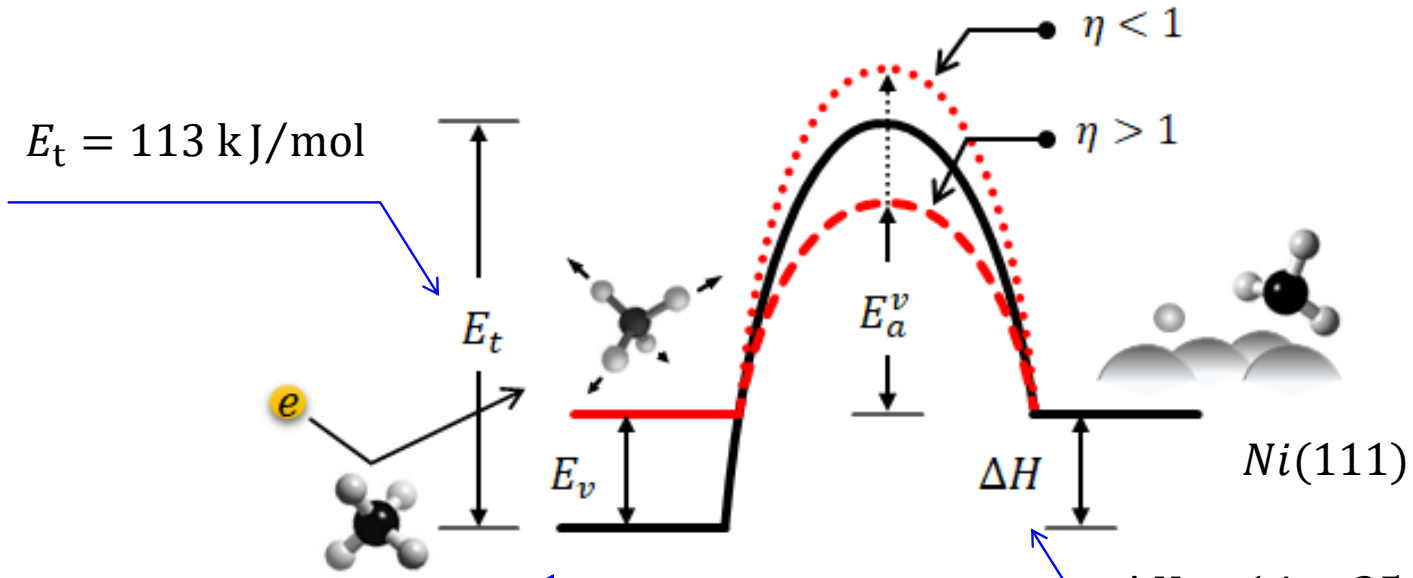

$E_t = 113\ \mathrm{kJ/mol}$

$E_v = 16 - 37\ \mathrm{kJ/mol}$

$\Delta H = 14 - 35\ kJ/mol$

$$k_f = Ae^{-\frac{E_t - \eta E_v}{RT}}$$

$$\eta = \frac{E_t - E_a^v}{E_v}$$

when $\eta = 1$, $\quad E_a^v = E_t - E_v$

Smith RR et al: *Science*, **304** (2004) 992.

S.-G. Wang et al, *Surface Science* **603** (2009) 2600-2606.

H. Liu et al, *Fuel* **113** (2013) 712-718.

Fundamental vibration mode of CH_4 and *Efficacy*

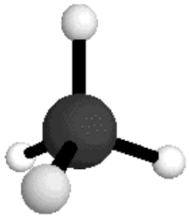

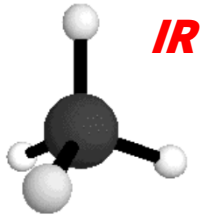

IR

Bending

ν_2 1582.7 cm^{-1}
E Symmetry

ν_4 1367.4 cm^{-1}
F2 Symmetry

[3]

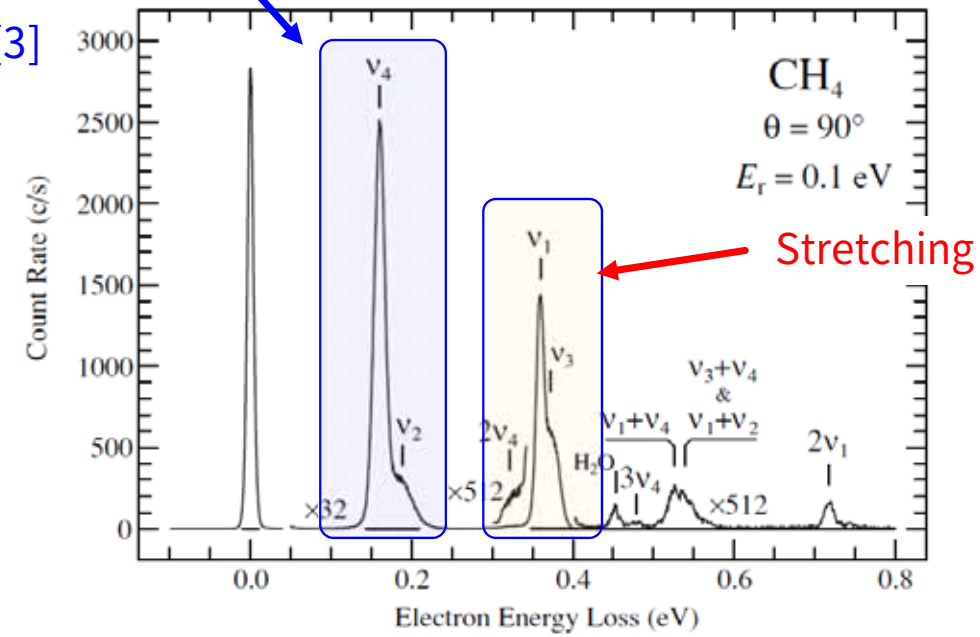

Stretching

[2]

State	E_{vib} kJ/mol	Surface	ΔE_{trans} kJ/mol	η_{vib}
CH_4, ν_3	36	Ni(100)	34 kJ/mol	0.94*
CH_4, $2\nu_3$	71	Ni(100)	68	0.96
CH_4, ν_1	35	Ni(100)	50	1.4*
CH_4, $3\nu_4$	45	Ni(100)	–	⩽0.5*
CH_4, ν_3	36	Ni(111)	45	1.25
CH_4, $2\nu_3$	71	Ni(111)	65	0.90
CH_4, $3\nu_4$	45	Ni(111)	34	0.72
CH_4, $2\nu_3$	71	Pt(111)	28	0.40
SiH_4, |2000>	53	Si(100) (1 × 2)	38	0.72*,†
SiH_4, |1100>	55	Si(100) (1 × 2)	22	0.40*,†

[1]

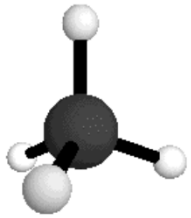

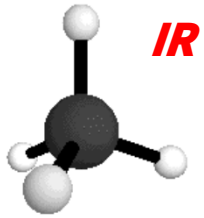

IR

ν_1 3025.5 cm^{-1}
A1 Symmetry

ν_3 3156.8 cm^{-1}
F2 Symmetry

[4] All Raman active. ν_3 and ν_4 are IR active.

1. http://www2.ess.ucla.edu/~schauble/
2. A.L. Utz: *Curr. Opin. Solid State and Mater. Sci.*, **13** (2009) 4–12.
3. M. Allan: *J. Phys. B: At. Mol. Opt. Phys.*, **38** (2005) 1679–1685.
4. Herzberg, G.: Molecular spectra and molecular structure. II. Infrared and Raman spectra of polyatomic molecules, 1939, Van Nostrand.

Modified activation energy : E_a^v

$$E_a^v = 91 - \eta E_v$$

Z Sheng et al, *Chem. Eng. J.*, **399** (2020) 125751.

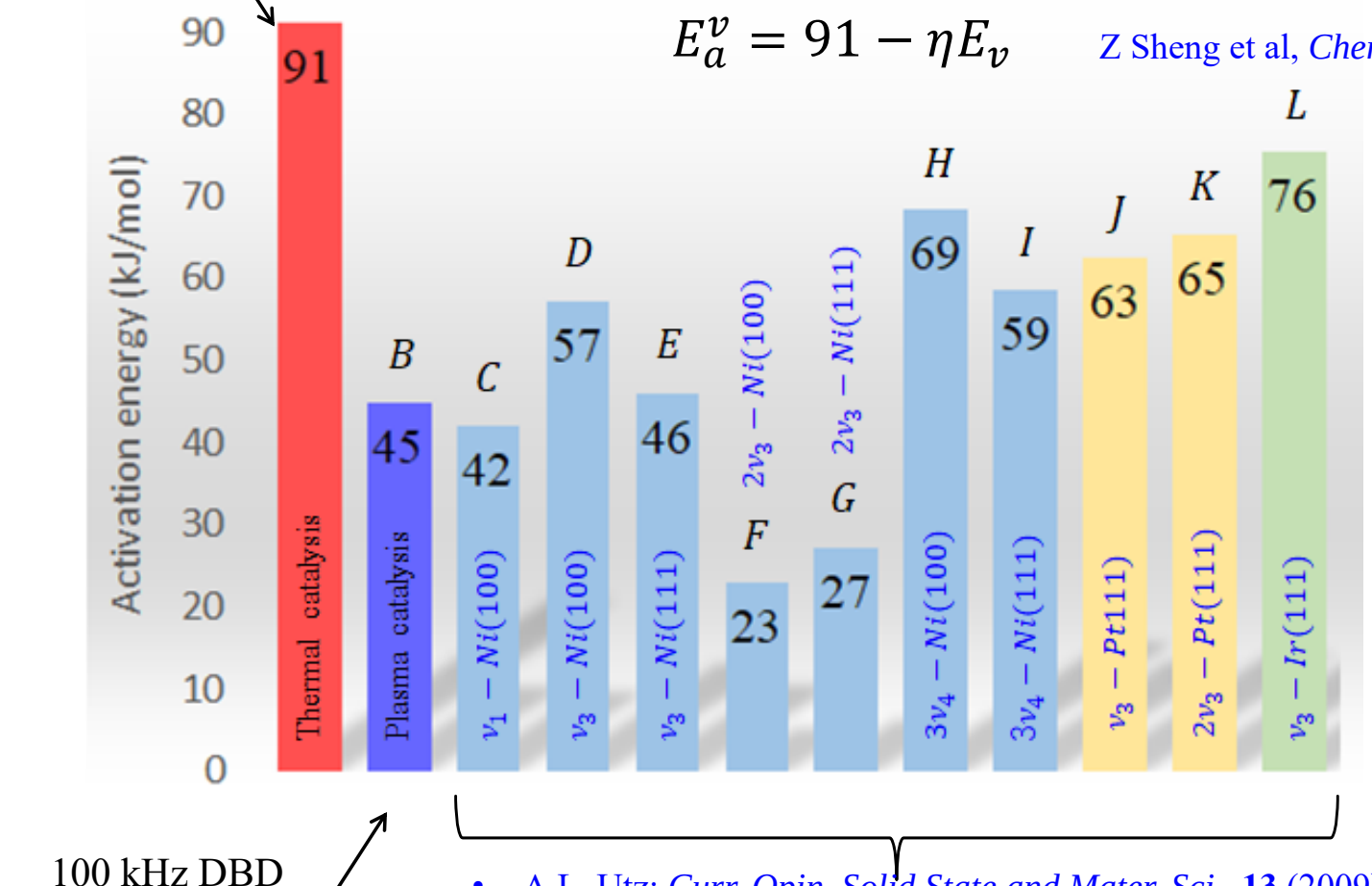

- A.L. Utz: *Curr. Opin. Solid State and Mater. Sci.*, **13** (2009) 4–12.
- H. Ueta et al, *Phys. Chem. Chem. Phys.*, **15** (2013) 20526-20535.
- R. Bisson et al, *J. Phys. Chem. A*, **111** (2007) 12679-12683.
- E. Dombrowski et al, *Catal. Today*, **244** (2015) 10-18.

V-V and V-T transition

Z Sheng et al, *Chem Eng. J.*, **399** (2020) 125751.

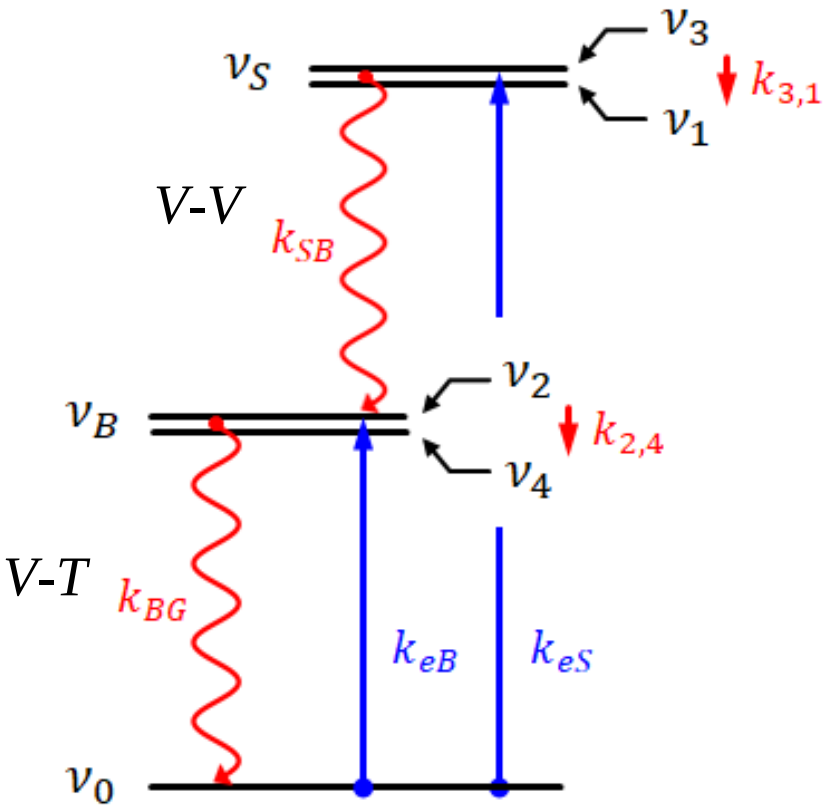

Reaction rate equation

$$\frac{dN_S}{dt} = k_{eS}N_{CH_4}N_e - k_{SB}(N_{CH_4} + N_{CO_2})N_S$$

BOLSIG+
5 kPa, 600 °C, $CH_4/CO_2 = 1$.

$(\tau_{st} = 10\ ns)$

$$\frac{dN_S}{dt} \approx -2k_{SB}NN_S \qquad t = 0, \quad N_{S0} = k_{eS}NN_e\tau_{st}$$

τ_{SB} (0.1 μs) < $T_{1/2}^{100kHz}$ (5 μs) < τ_{BG} (31 μs) < $T_{1/2}^{12kHz}$ (42 μs)

DBD generation cycle is 6-time faster than V-T transition.
Bending mode $CH_4(\nu_4)$ would be populated.
Generation of combined/overtone vibration mode (e.g. $3\nu_3$) is necessary.

$$CH_4(\nu_B) + e \rightarrow CH_4(\nu_S + \nu_B) + e$$

$$CH_4(\nu_S + \nu_B) + CH_4 \leftrightarrow CH_4(3\nu_B) + CH_4$$

Discharge behavior of PB-DBD

Why 100 kHz DBD is superior to 12 kHz DBD?

Discharge power and controlling parameters

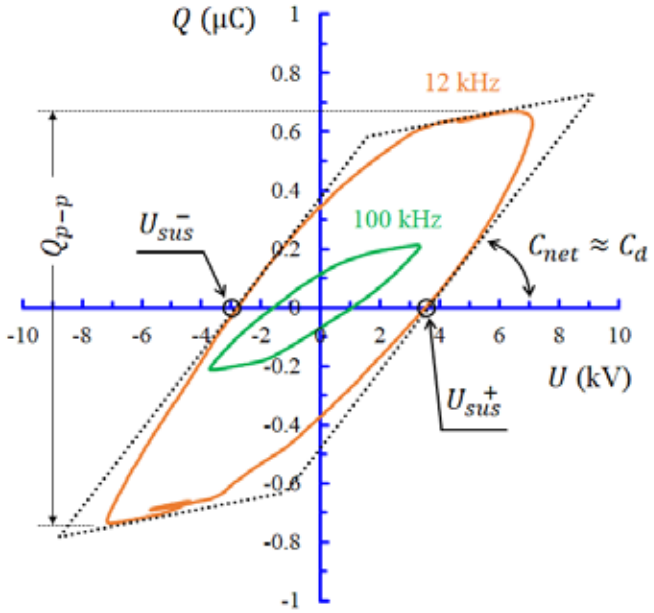

$$P_L = f \oint Q dU$$

$Q_{p\text{-}p}$: peck-to-peck value of charge

U_{sus}: discharge sustain voltage

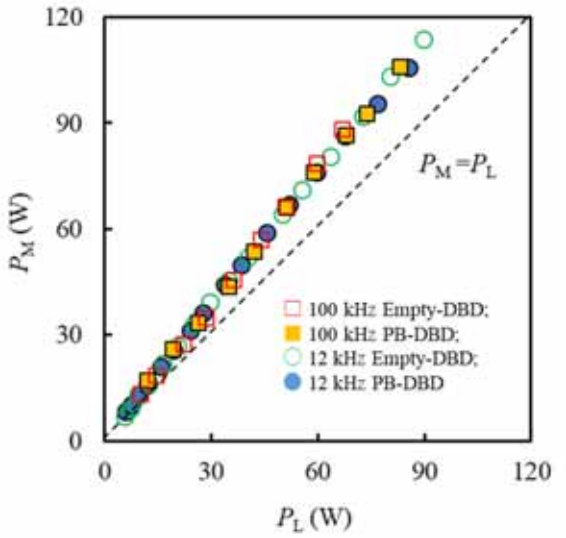

100 kHz Empty-DBD

12 kHz Empty-DBD

100 kHz PB-DBD

12 kHz PB-DBD

Manley's equation

T C Manley, *Trans. Electrochem. Soc.*, **84** (1943) 93–96

$$P_M = 4f\bar{U}_{sus}\frac{Q_{p-p}}{2} = 4\bar{U}_{sus}\frac{I_{p\_p}}{2} \qquad (C_{die} \gg C_{gas})$$

See also, Xin Tu et al, Plasma Catalysis: Fundamentals and Applications, *Springer*, 2019, pp.231-269.

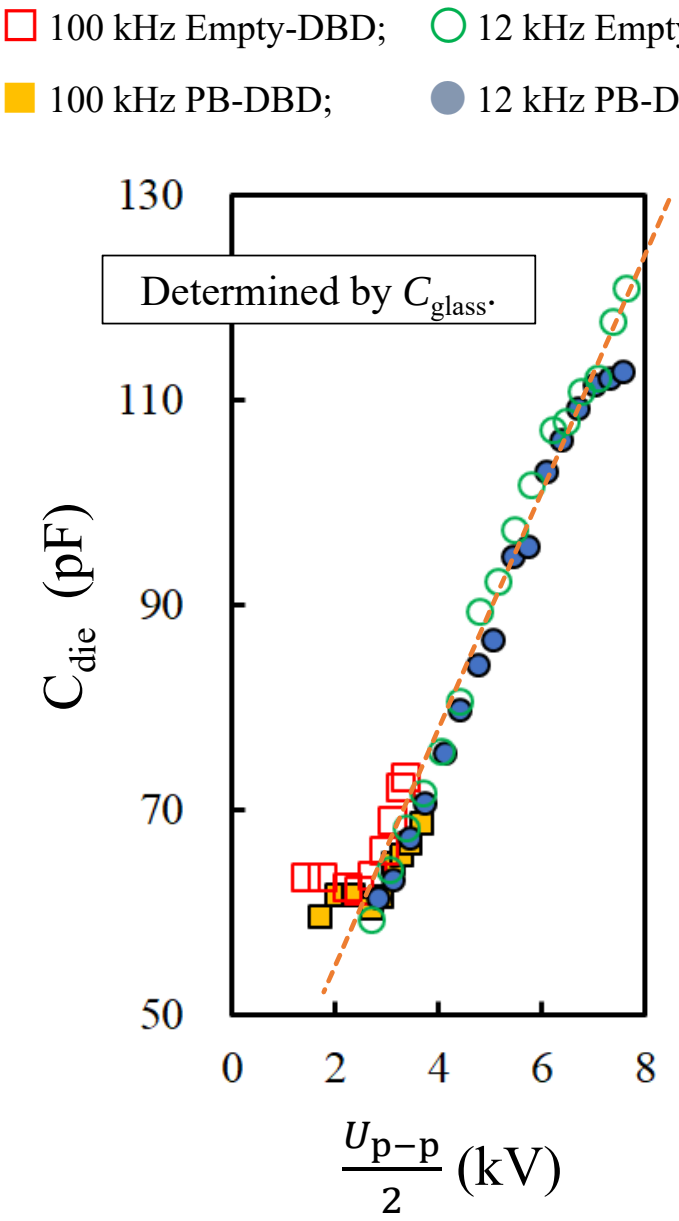

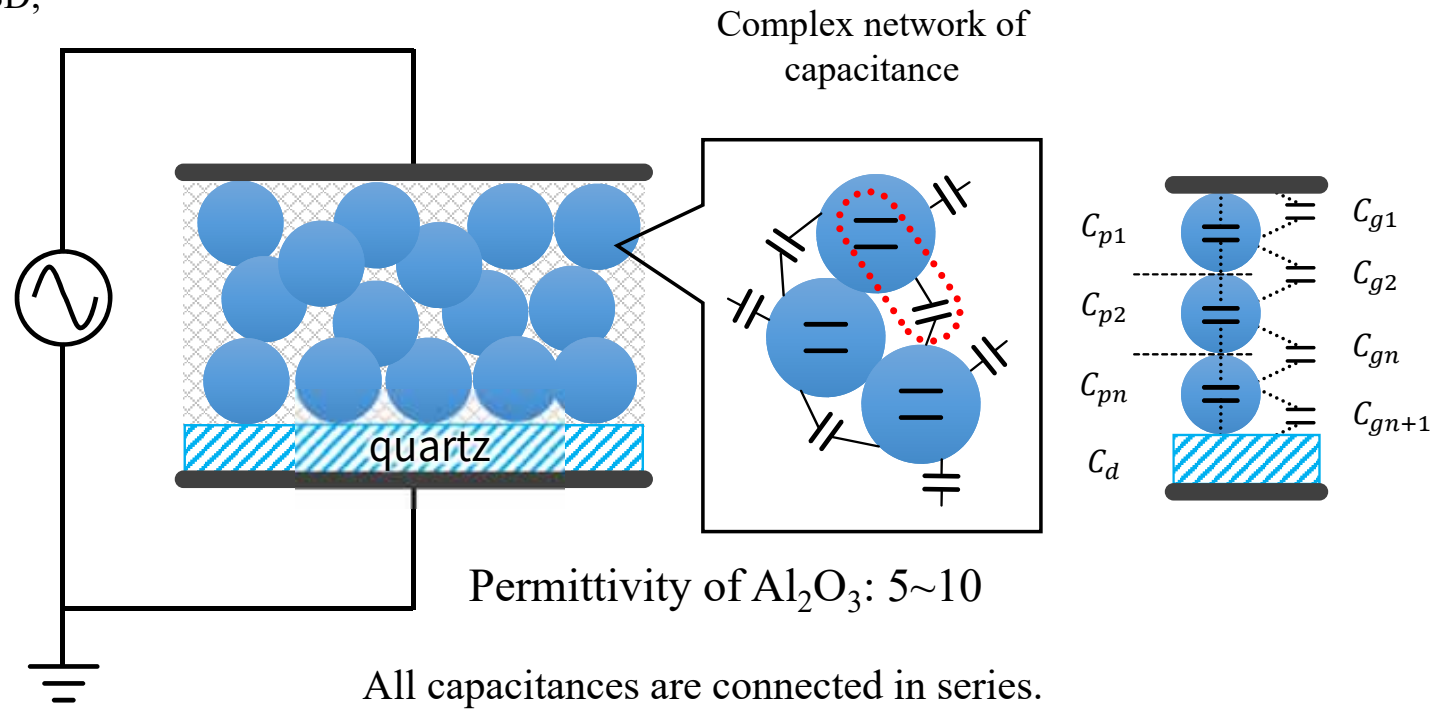

Permittivity of Al_2O_3: 5~10

All capacitances are connected in series.
Gas gap between pellets cancels the capacitance of catalysts

Why no effect of pellets?

T. Butterworth et al, *Chem. Eng. J.* **293** (2016) 55–67.

- Pressure is "5 kPa" --- DBD would be diffused and decoupled with dielectric properties.
- Metal loading change streamer propagation.

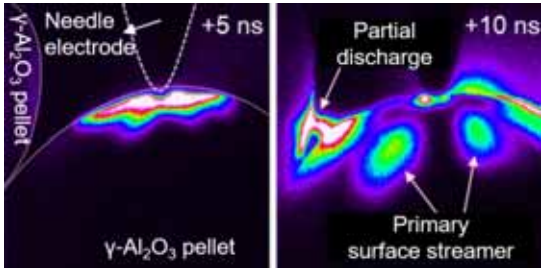

H-H Kim et al: *J Phys D*, **49** (2016) 315204

Additional info

$$\frac{I_{p-p}}{2} = f\frac{Q_{p-p}}{2}$$

per cycle properties

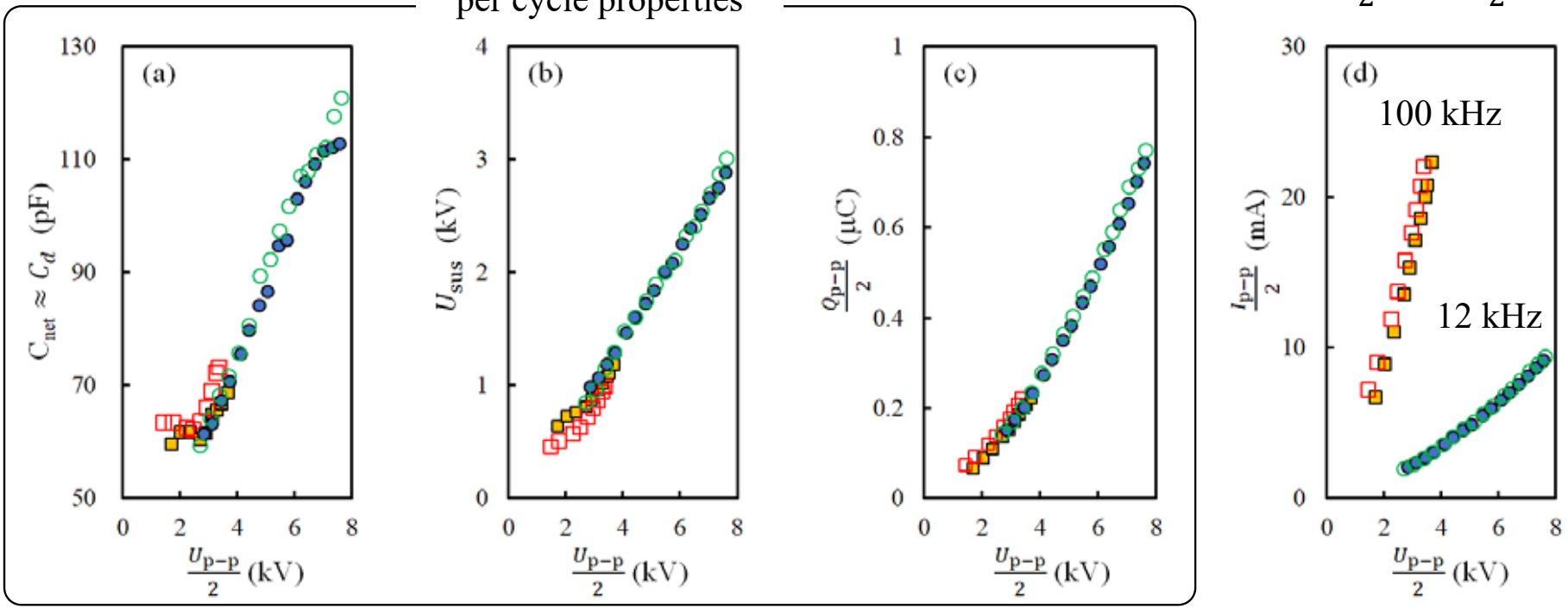

- Discharge current increases doubled by frequency, while keeping the same power: Minimize heating effect and enhancing radical production rate.
- If the electric charge would increase with pellets ... we need a large power source to drive DBD!

What is the properties of individual streamer?

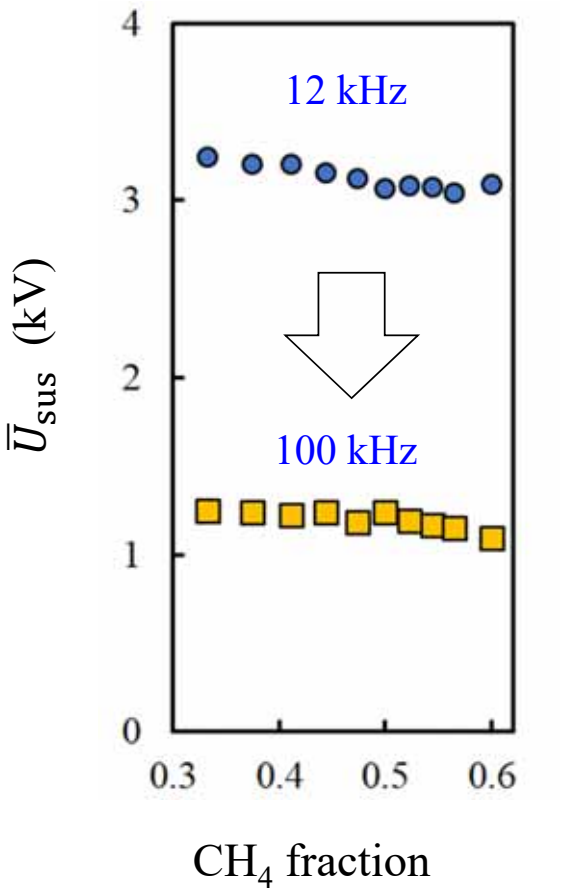

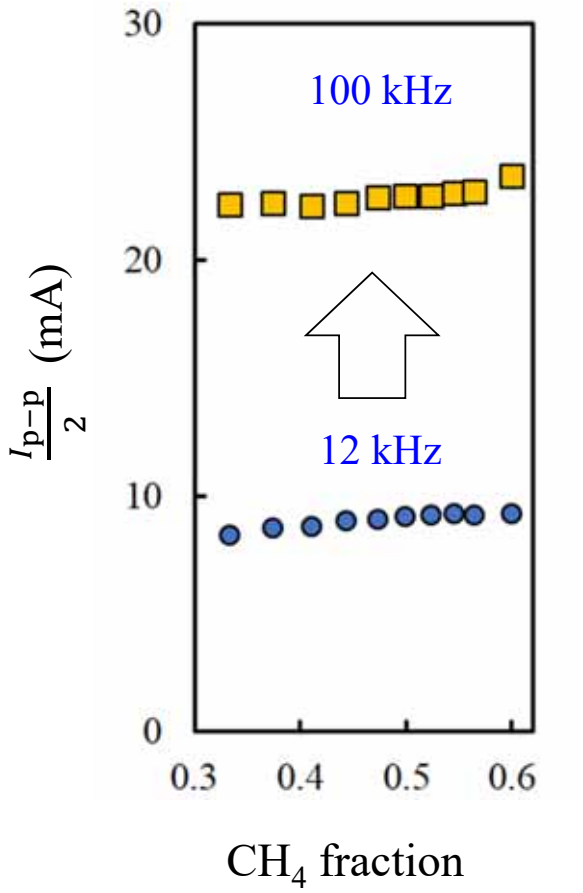

Manley's equation

$$P_M = 4f\bar{U}_{sus}\frac{Q_{p-p}}{2} = 4\bar{U}_{sus}\frac{I_{p-p}}{2} \quad (C_{die} \gg C_{gas})$$

100 kHz DBD generates more streamers per unit time.

Per streamer

$$\frac{\mathrm{d}CH_4^v}{\mathrm{d}t} = k_v N_{CH_4} N_e$$

$$\Delta CH_4^v / N_e = 40 - 150$$

Z Sheng, *Chem. Eng. J.*, **399** (2020) 125751.

T Nozaki, *Catal. Today*, **89** (2004) 57-65.

What is the discharge properties of individual streamer?

BOLSIG+ $CH_4/CO_2 = 1$; 5 kPa; 600 °C

Reduced electric field

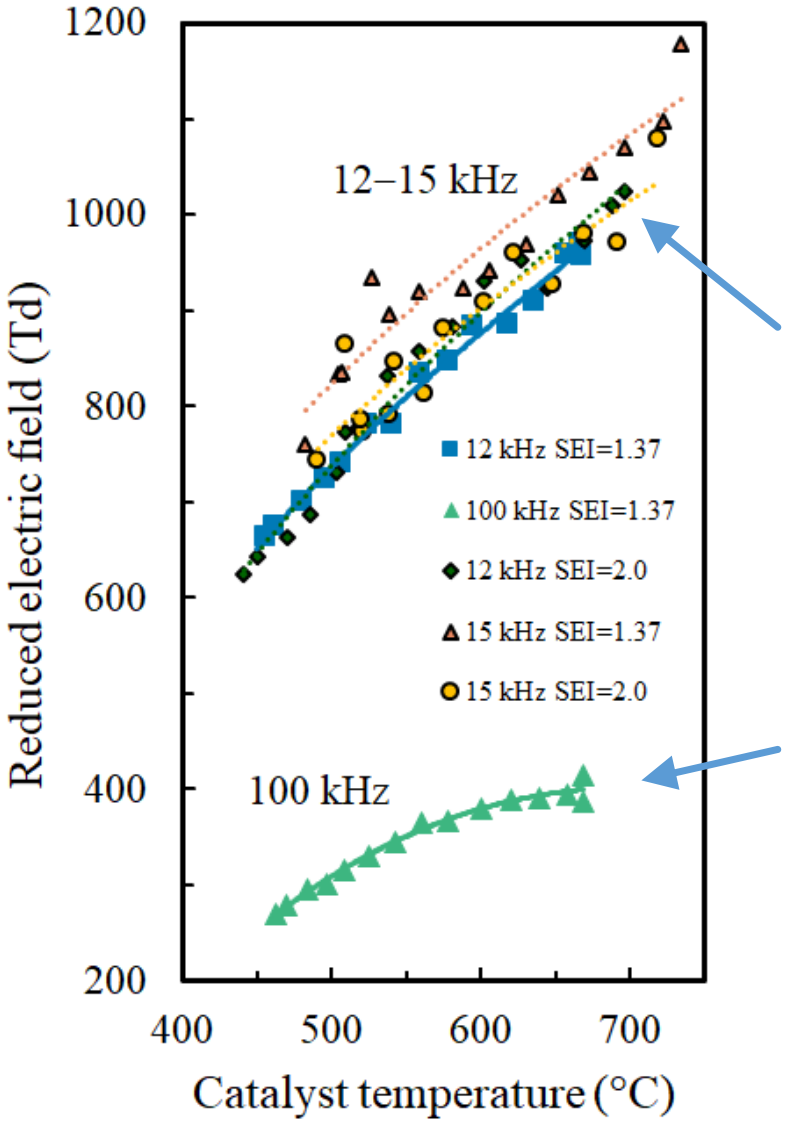

Reduced electric field

$$\frac{E}{N}(Td) = \frac{U_{sus}}{d \times N}$$

12 kHz

- High-Td regime
- Discharge properties do not change by *SEI* or *GHSV*.

100 kHz

- Low-Td regime
- Discharge properties are distinguished from 12 kHz DBD.

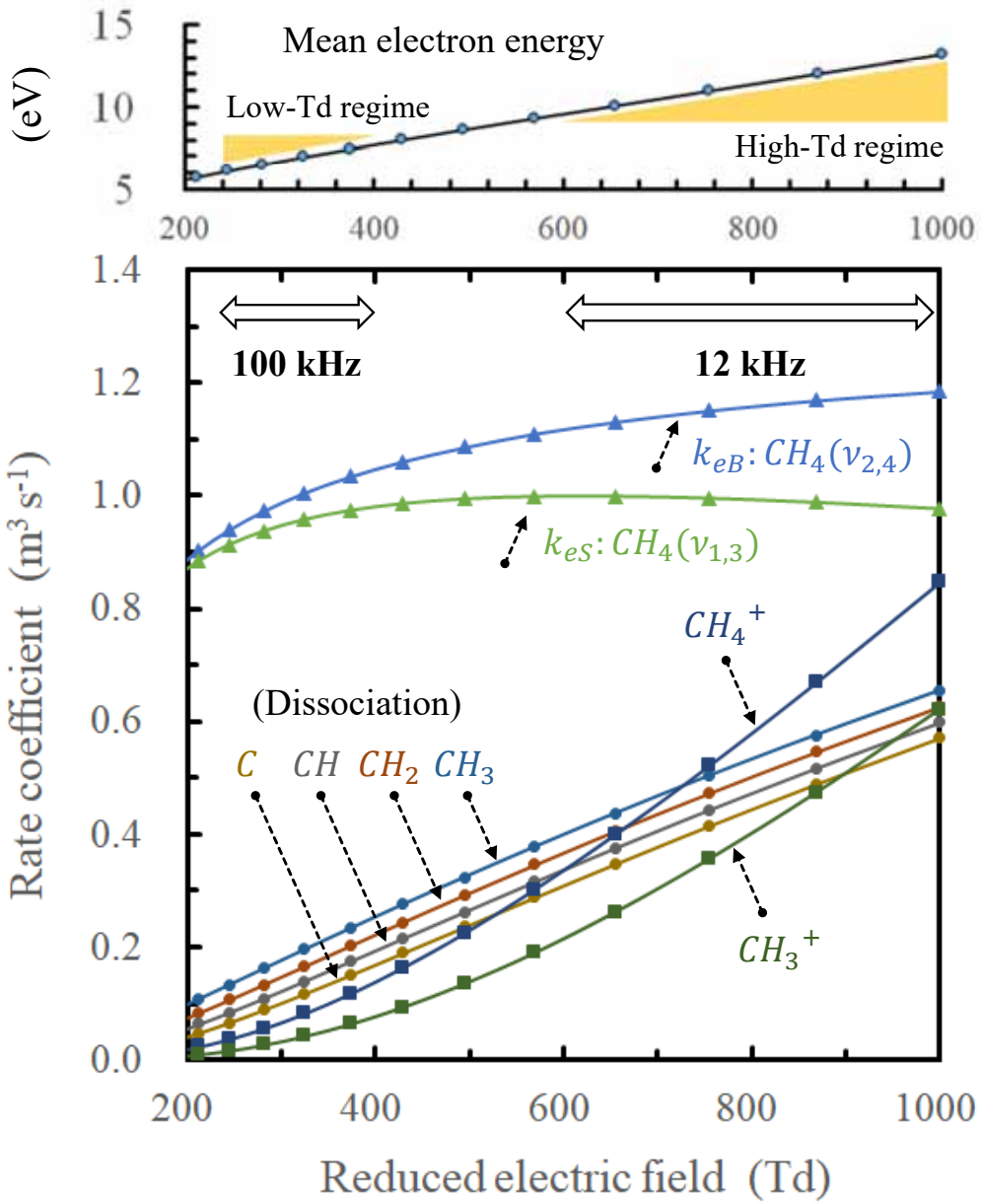

← Z Sheng, *Chem. Eng. J.*, **399** (2020) 125751.

↓ T Nozaki, *Catal. Today*, **89** (2004) 57-65.

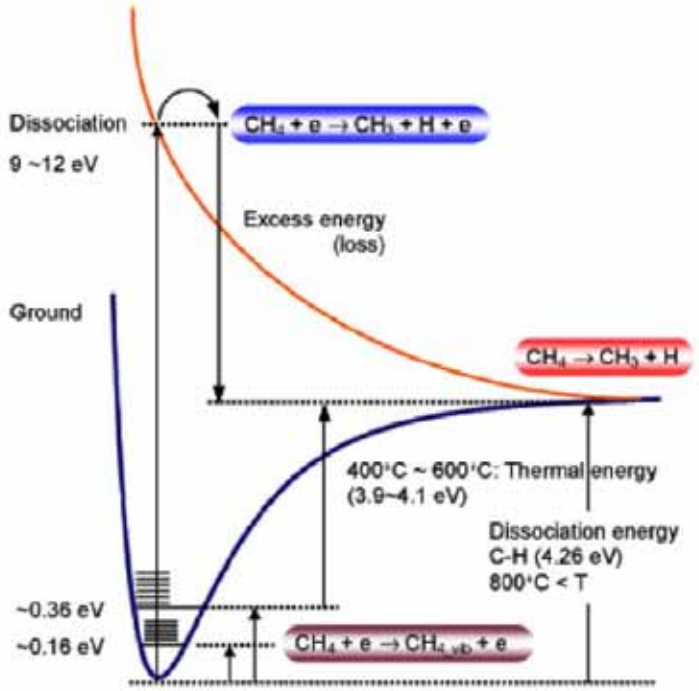

Arrhenius plot for different *SEI* and *GHSV*

Blue symbol: *SEI* 1.37, *GHSV* 5,144, 90 W, 1000 cm^3/min

GHSV decreases, SEI oncreases

SEI 1.37, *GHSV* 10,289
180 W, 2000 cm^3/min

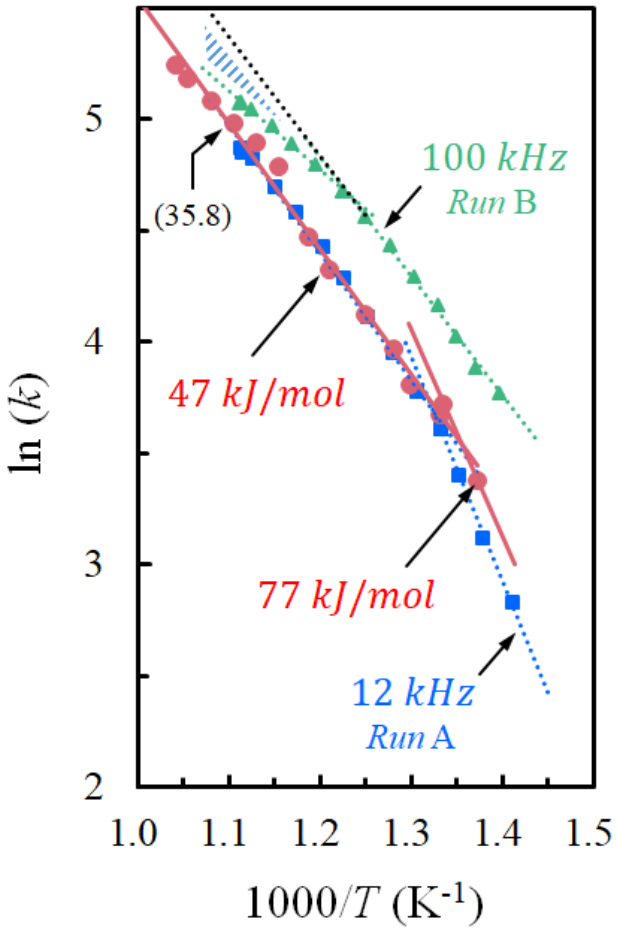

SEI 2.0, *GHSV* 5,144
130 W, 1000 cm^3/min

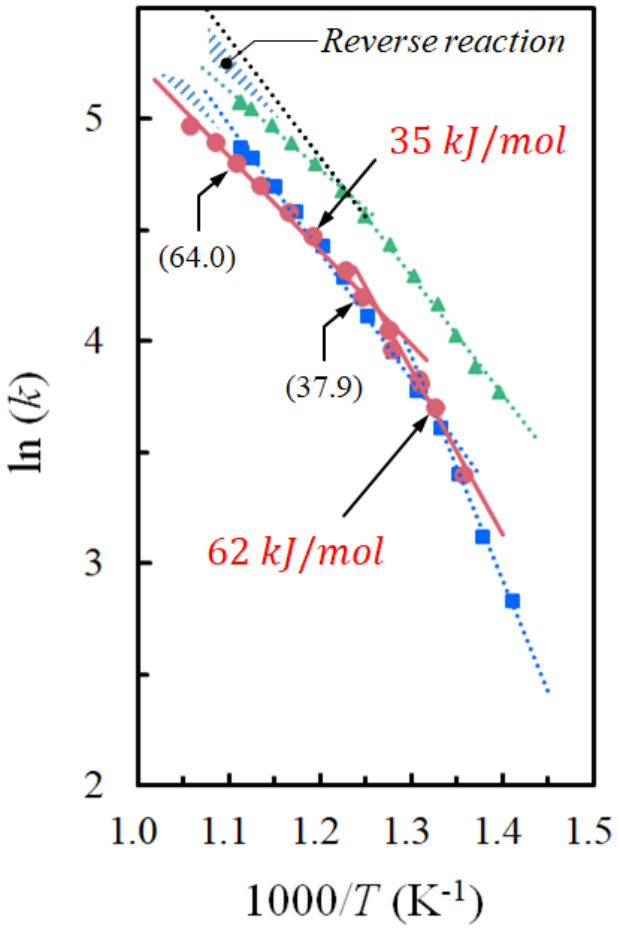

SEI 2.0, *GHSV* 3,600
90 W, 700 cm^3/min

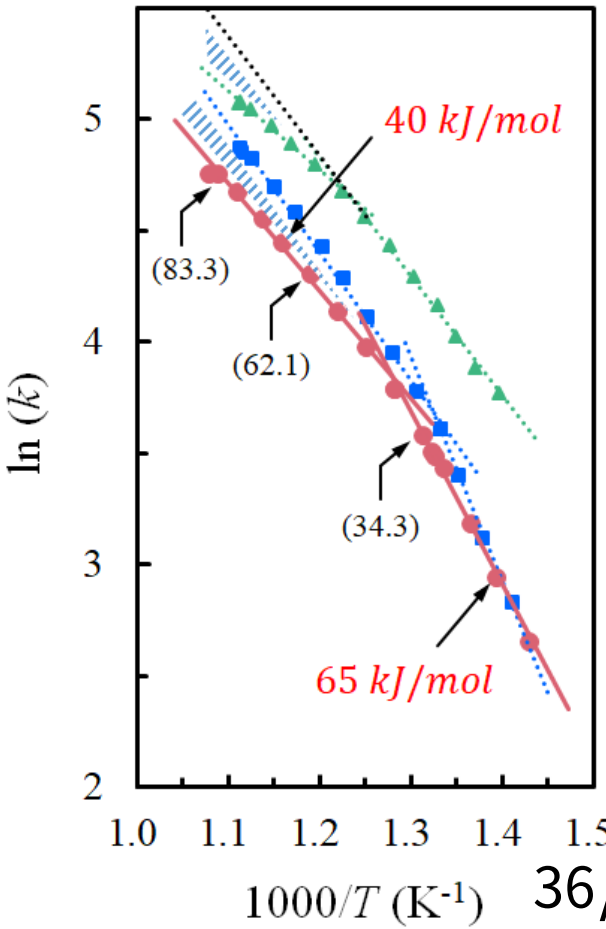

CH_4 conversion increases with *SEI* and Reaction time ($GHSV^{-1}$).

→ Do kinetic parameters change --- perhaps not !

1. *GHSV* decreases, conversion increases:

→ conversion per reaction time (reaction rate) is constant.

2. E/N does not change by *SEI* or *GHSV*.

→ A number of streamers changes, but streamer properties do not change to a large extent.

→ Activation energy is independent of *SEI* and *GHSV* at fixed frequency

Frequency (kHz)	U_{sus} (kV)	$I_{p\text{-}p}/2$ (mA)	Power (W)	Total flow (cm^3/min)	*SEI*	*GHSV*
12 (control)	$3.03^{+0.16}_{-0.21}$	$9.18^{+0.61}_{-0.47}$	90	1,000	1.37	5,144
15	$3.37^{+0.23}_{-0.27}$	$14.1^{+0.75}_{-0.74}$	180	2,000	1.37	10,289
15	$3.15^{+0.25}_{-0.15}$	$12.5^{+1.27}_{-1.17}$	130	1,000	2.0	5,144
12	$3.05^{+0.23}_{-0.35}$	$9.19^{+0.67}_{-0.94}$	90	700	2.0	3,600

ex. CH_4 steam reforming $CH_4 + 2H_2O = CO_2 + 4H_2$

T Nozaki et al: *Energy & Fuels*, **21**, 2525, 2007.

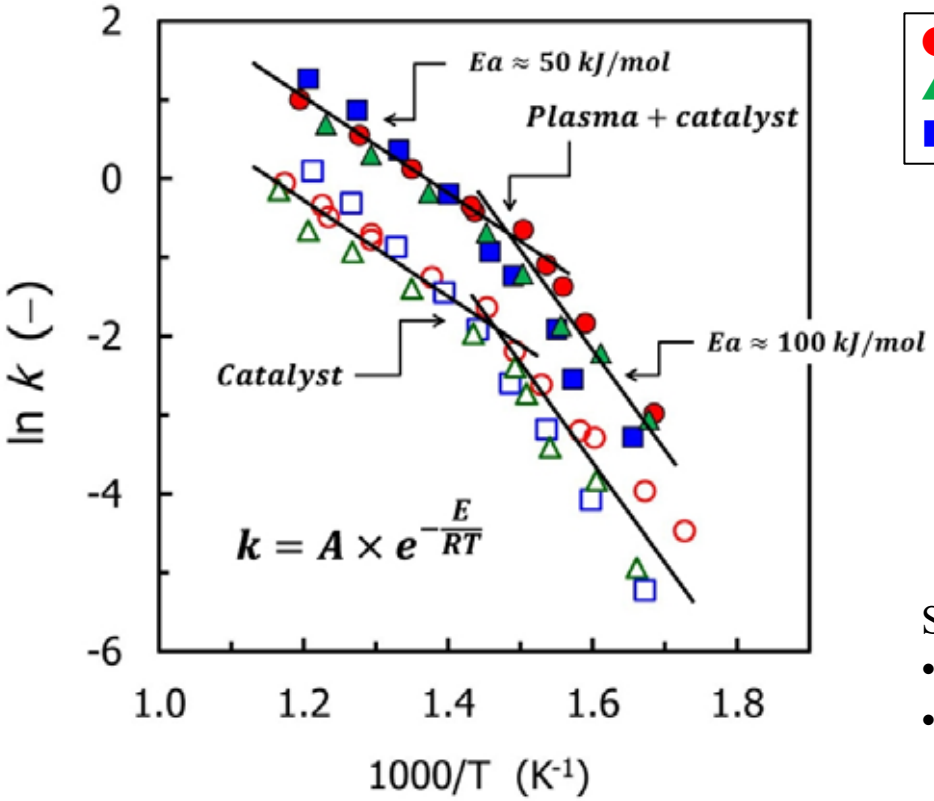

● ○ : S/C = 1, GHSV = 18,000 hr^{-1}
▲ △ : S/C = 3, GHSV = 18,000 hr^{-1}
■ □ : S/C = 1, GHSV = 10,000 hr^{-1}

Conditions:
- $Ni(12wt\%)/Al_2O_3$ catalysts.
- 1–5 kHz bipolar pulsed high voltage.
- *SEI* = 0.22–0.36 eV/molecule.
- 101 kPa (N_2 dilution).
- $E_t \approx 100$ kJ/mol (T_B = 420 °C).

Similar kinetic behavior:
- Reaction order was unaffected by DBD
- Activation energy was unaffected by DBD, but reaction rate constant increased by DBD.

Conclusions

Please consult the *Figures* and *Statements* on Page 7, 10, 23, 26, 30, and 37.

Related to this presentation

- Z Sheng et al, *Journal of Physics D: Applied Physics*, **52**,414002(13pp), 2019.
- Z Sheng et al, *Physical Chemistry Chemical Physics*, **22**, 19349-19358, 2020.
- Z Sheng et al, *Chemical Engineering Journal*, **399**, 125751(14pp), 2020.

The 2020 Plasma Catalysis Roadmap

- A Bogaerts, X Tu, et al: *J. Phys. D: Appl. Phys.*, **53** (2020) 443001(51pp).

Acknowledgements

- Dr. Hyun-Ha Kim, AIST, Japan.
- Dr student, Zunrong Sheng, Tokyo Tech
- Dr. H. Ueta, Japan Atomic Energy Agency

- JST CREST (JPMJCR19R3)

Gas temp. ≈ Catalyst temp.

P Bruggeman, T Nozaki et al, *Plasma Chem. Plasma Process.*, **37** (2017) 29–41.

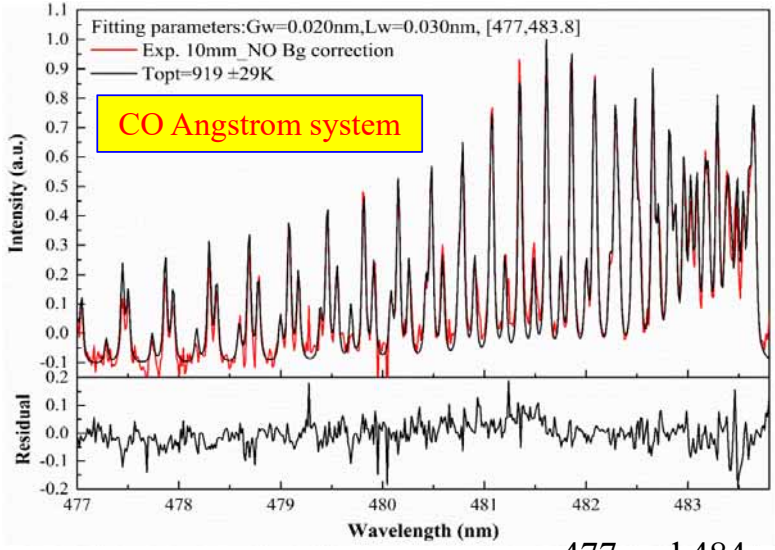

477 and 484 nm.

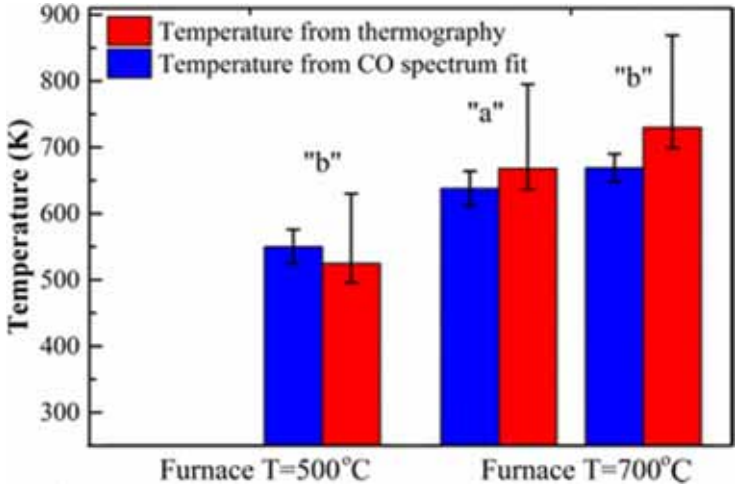

Optical emission

H-H Kim et al: *J Phys D*, **49** (2016) 415204

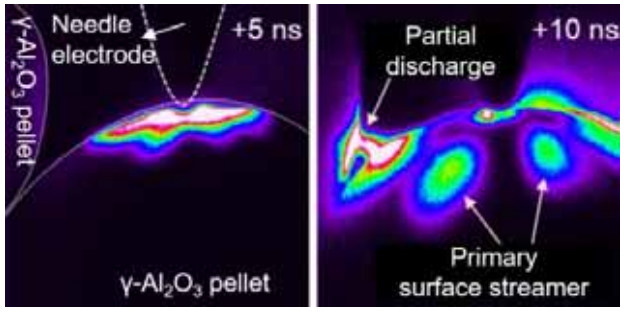

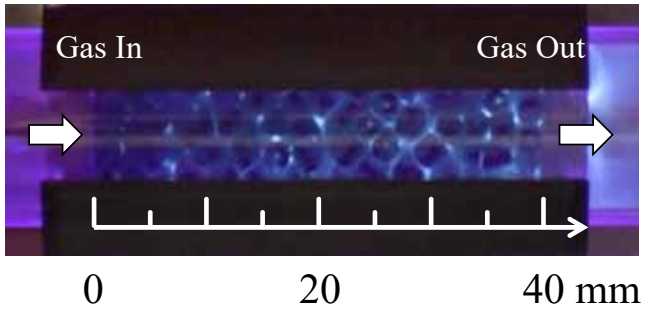

DBD: Dielectric Barrier Discharge

Reaction orders